CP-violating observables in four-body $B \to \phi(\to K\bar{K})K^*(\to K\pi)$ decays

Chao-Qi Zhang,[1] Jia-Ming Li,[1] Meng-Kun Jia,[1] Ya Li,[2,*] and Zhou Rui[1,†]

[1]*College of Sciences, North China University of Science and Technology, Tangshan, Hebei 063210, China*
[2]*Department of Physics, College of Science, Nanjing Agricultural University, Nanjing, Jiangsu 210095, China*

(Received 26 December 2021; accepted 18 February 2022; published 9 March 2022)

We analyze the four-body $B \to \phi(\to K\bar{K})K^*(\to K\pi)$ decays in the perturbative QCD approach, where the invariant mass of the $K\bar{K}$ ($K\pi$) system is limited in a window of ± 15 MeV (± 150 MeV) around the nominal $\phi(K^*(892))$ mass. In addition to the dominant P-wave resonances, two important S-wave backgrounds in the selected invariant mass region are also accounted for. Angular momentum conservation allows six helicity amplitudes to contribute, including three P waves, two single S waves, and one double S wave, in the decays under study. We calculated the branching ratio for each component and found sizable S-wave contributions, which coincide roughly with the experimental observation. The obtained branching ratios of $B^{0(+)} \to \phi K^{*0(+)}$ are comparable with the previous theoretical predictions and support the experimental measurements, whereas the predicted $\mathcal{B}(B_s^0 \to \phi\bar{K}^{*0})$ is an order of magnitude smaller than the current world average in its central value. The longitudinal polarizations are predicted to be around 0.7, consistent with previous PQCD results but larger than the world average values. Aside from the direct CP asymmetries, the true and fake triple product asymmetries, originating from the interference between the perpendicular polarization amplitude and other helicity amplitudes, are also calculated in this work. In the special case of the neutral modes, both the direct CP asymmetries and true triple product asymmetries are expected to be zero due to the vanishing weak phase difference. The direct CP asymmetries for the B^+ mode are predicted to be tiny, of order 10^{-2}, since the tree contributions are suppressed strongly with respect to the penguin ones. The true triple product asymmetries have shown no significant deviations from zero. In contrast, large fake asymmetries are observed in these decays, indicating the presence of significant final-state interactions. We give the theoretical predictions of the S-wave induced triple product asymmetries for the first time, which is consistent with current LHCb data and would be checked with future measurements from Belle and *BABAR* experiments if the S-wave components can be properly taken into account in the angular analysis.

DOI: 10.1103/PhysRevD.105.053002

I. INTRODUCTION

The phenomenology of B decays to two light vector mesons provides unique opportunities for understanding the mechanism of hadronic weak decays and their CP asymmetry, and probing the new physics (NP) beyond the standard model (SM). Angular momentum conservation leads to three independent configurations of the vector mesons which reflects into three amplitudes. In the transversity basis, the decay amplitude can be decomposed into three independent components A_0, $A_\parallel$, and $A_\perp$ [1,2], which correspond to longitudinal, parallel, and perpendicular polarizations of the final-state spin vectors, respectively. Experimentally they are at least four-body decays [3], since a vector resonance is usually detected via its decay $V \to PP'$ with $P^{(\prime)}$ being a pseudoscalar. As the vector meson has a relatively broad width, there is generally a background due to the (resonant or nonresonant) scalar production of the two pseudoscalars [4,5] around the vector resonance region. In this case, it is necessary to add another three scalar amplitudes to the angular analysis in the presence of the scalar background [6]. Then one can extract more CP-violating observables from the interference of the various helicity amplitudes. Therefore, the four-body charmless B decays through two vector intermediate states are rich in CP-violating phenomena in the flavor sector involving quarks.

A four-body decay gives rise to three independent final momenta $\vec{p}_i$ with $i = 1, 2, 3$ in the rest frame of the decaying parent particle, and allows one to form a scalar

*Corresponding author.
liyakelly@163.com
†Corresponding author.
jindui1127@126.com

triple product (TP) of $\vec{p}_1 \cdot (\vec{p}_2 \times \vec{p}_3)$. Obviously, it is odd under both parity and time reversal, and thus constitutes a potential signal of CP violation assuming CPT invariance. One can compare event distributions for positive TP against those with negative TP to construct a triple product asymmetry (TPA),

$$A_T \equiv \frac{\Gamma(TP>0)-\Gamma(TP<0)}{\Gamma(TP>0)+\Gamma(TP<0)}, \tag{1}$$

where Γ is the partial decay rate in the indicated TP range. However, since both the final-state interaction and CP violation can produce the nonzero TPAs, one has to compare this asymmetry with a corresponding quantity in the CP conjugate process to obtain the "true" CP violation signal. Furthermore, unlike the direct CP violation, a nonzero true TPA does not require the presence of a nonzero strong phase [7], while it is maximal when the strong phase difference vanishes. In this case, it could be more promising to search for TPA than direct CP asymmetries in B decays. Therefore, the TPA is one powerful tool for displaying CP violation in weak four-body decays [8,9]. Further information on this rich subject may be found in Refs. [6–14].

Four-body decays of the B meson are more complicated than the two-body case, specifically where both nonresonant and resonant contributions exist. In our previous works [15,16], the PQCD factorization formalism based on the quasi-two-body decay mechanism [17–19] for four-body B meson decays has been well established. That is, a four-particle final state is obtained through two intermediate resonances. The resonances decaying into the meson pair are modeled by nonperturbative two-hadron distribution amplitudes (DAs) [20–26], which collect both resonant and nonresonant contributions [27]. In this work, a similar strategy is extended to the penguin-dominated four-body decays $B \to \phi(\to K\bar{K})K^*(\to K\pi)$, which exhibit particularly alluring experimental and theoretical features.

In the SM, the decay $B \to \phi K^*$ is described by loop mediated $b \to d$ or $b \to s$ transitions, providing a sensitive test for NP. The $B^0 \to \phi K^{*0}$ decay was first observed by the CLEO Collaboration [28]. Subsequently, branching ratio measurements and angular analyses have been reported by the *BABAR* and Belle Collaborations [29–36]. The branching ratio as averaged by the Particle Data Group (PDG) is $(1.00 \pm 0.05) \times 10^{-5}$ [37], in good agreement with theoretical predictions [38,39]. The observed surprisingly large transverse polarization fractions, contrary to naive predictions based on helicity arguments (the so-called polarization puzzle [37]), attracts much theoretical attention, with several explanations proposed [40–57]. Including both the S-wave $K^+\pi^-$ and K^+K^- contributions, the LHCb Collaboration measured the polarization amplitudes and CP asymmetries in $B^0 \to \phi(\to K^+K^-)K^{*0}(\to K^+\pi^-)$ decay [58]. The angular analysis was used to determine TPAs for the first time. The measured true asymmetries show no significant deviations from zero, while several significant fake TPAs are consistent with the presence of final-state interactions. As for the B_s counterpart, the first observation of the decay $B_s^0 \to \phi\bar{K}^{*0}$, with $\phi \to K^+K^-$ and $\bar{K}^{*0} \to K^-\pi^+$, was reported by the LHCb experiment [59], meanwhile, the determination of its branching ratio and polarizations were presented, and the S-wave contribution was estimated to be in the teens. The measured value of the branching ratio is significantly larger than the theoretical predictions [38,60–65].

As discussed above, we focus on the four-body decays $B \to \phi(\to K\bar{K})K^*(\to K\pi)$, where the invariant mass of the $K\bar{K}$ ($K\pi$) pair is restricted to be within ± 15 MeV (± 150 MeV) of the known mass of the $\phi(K^*(892))$ meson for comparison with the LHCb data. Except for the dominant vector resonances, two important scalar backgrounds, such as $f_0(980) \to K\bar{K}$ and $K_0^*(1430) \to K\pi$, are also taken into account. The contributions from higher spin resonances are expect to be small in the concerned mass regions and are thus neglected in the following analysis. Six different quasi-two-body decay channels are considered, corresponding to various different possible combinations of $K\bar{K}$ and $K\pi$ pairs with spin 0 and 1. The S and P-wave contributions are parametrized into the corresponding timelike form factors involved in the two-meson DAs, which are well established in the three-body B decays [66,67]. With these universal nonperturbative quantities, we can make quantitative predictions on the various observables including the branching ratios, S-wave fractions, polarization fractions, direct CP violations, and the TPAs in $B \to \phi(\to K\bar{K})K^*(\to K\pi)$ decays.

The rest of the paper is organized as follows. Section II includes a general description of the angular distribution, kinematics, and the two-meson distribution amplitudes of the considered four-body decays. We then apply the PQCD formalism in Sec. III to the $B \to \phi(\to K\bar{K})K^*(\to K\pi)$ decays. The numerical results are discussed and compared with those of other works in the literature. Section IV contains our conclusions. The relevant factorization formulas are collected in the Appendix.

II. KINEMATICS AND TWO-MESON DISTRIBUTION AMPLITUDES

A. Angular distribution and the helicity amplitudes

The angular distribution in the $B^0 \to \phi K^{*0}$ decay with $\phi \to K^+K^-$ and $K^{*0} \to K^+\pi^-$ is described by three angles θ_1, θ_2, and ϕ in the helicity basis, which are depicted in Fig. 1. θ_1 is the polar angle of the K^+ in the rest frame of the K^* with respect to the helicity axis. Similarly, θ_2 is the polar angle of the K^+ in the ϕ rest frame with respect to the helicity axis of the ϕ. The azimuth angle φ is the relative angle between the K^+K^- and $K^+\pi^-$ decay planes in the B rest frame.

Angular momentum conservation, for the vector-vector modes, allows three possible polarization configurations of the $K\bar{K}$ and $K\pi$ pairs, such as longitudinal, parallel, or

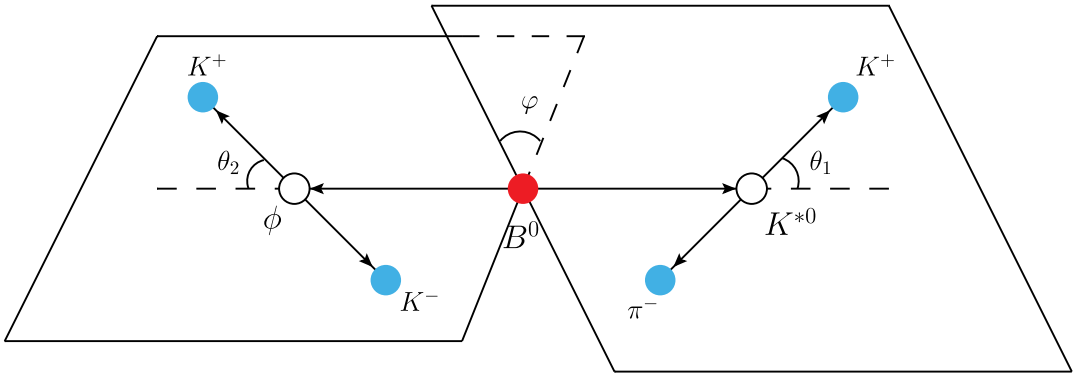

FIG. 1. The definition of the decay angles θ_1, θ_2, and φ for the decay $B^0 \to \phi K^{*0}$ with $\phi \to K^+K^-$ and $K^{*0} \to K^+\pi^-$. The angles are described in the text.

perpendicular. The corresponding amplitudes are denoted by A_0, $A_\parallel$, and $A_\perp$ respectively, following the definitions given in Ref. [15]. Some scalar resonances, such as $f_0(980)$ and $K_0^*(1430)$, are expected to contribute and thus are included in the selected region of $K\bar{K}$ or $K\pi$ invariant masses. As one of the meson pair is produced in a spin-0 (S-wave) state, the resultant two single S-wave amplitudes are denoted as A_{SV} and A_{VS}, which are physically different. The double S-wave amplitude A_{SS} is associated with the final state, where both meson pairs are produced in the S wave. All of the above considered decay modes, together with the corresponding amplitudes, are shown in Table I.

As discussed in Ref. [15], in the PQCD approach, these helicity amplitudes are expressed as the convolution of the hard kernels with the two-meson DAs, which absorb the nonperturbative dynamics involved in the meson pairs. After regularizing the end-point singularities and smearing the double logarithmic divergence, the typical factorization formula in coordinate space reads as

$$\begin{aligned} A \propto & \int dx_B dx_1 dx_2 b_B db_B b_1 db_1 b_2 db_2 \\ & \times \mathrm{Tr}[C(t)\Phi_B(x_B, b_B)\Phi_{K\pi}(x_1) \\ & \times \Phi_{K\bar{K}}(x_2) H(x_i, b_i, t) S_t(x_i) e^{-S(t)}], \end{aligned} \tag{2}$$

where x_i and b_i with $i = B, 1, 2$ are the parton momentum fractions and the conjugate space coordinate of the transverse momentum, respectively. The threshold function $S_t(x_i)$ and the Sudakov exponents $S(t)$ are given in the Appendix of Ref. [15]. t is the largest energy scale in hard function H. $C(t)$ is the short distance Wilson coefficients at the hard scale t. "Tr" denotes the trace over all Dirac structure and color indices. The explicit analytic formulas for the considered helicity amplitudes are presented in the Appendix.

TABLE I. Quasi-two-body decay channels and the corresponding helicity amplitudes contributing to the $(K\bar{K})(K\pi)$ final state. The subscript S/P denotes an S- or P-wave configuration of the meson pair.

Quasi-two-body modes	Resonance types	Allowed helicity amplitudes
$B \to (K\bar{K})_P(K\pi)_P$	Vector-vector	$A_{0,\parallel,\perp}$
$B \to (K\bar{K})_S(K\pi)_P$	Scalar-vector	A_{SV}
$B \to (K\bar{K})_P(K\pi)_S$	Vector-scalar	A_{VS}
$B \to (K\bar{K})_S(K\pi)_S$	Scalar-scalar	A_{SS}

B. The kinematics of four-body decay

Taking the full cascade decay $B \to \phi(\to K\bar{K})K^*(\to K\pi)$ as an example, the kinematics can be described in terms of five independent variables: three helicity angles $(\theta_1, \theta_2, \varphi)$ and two invariant masses $(m_{KK}, m_{K\pi})$. We first consider the subprocess $B \to \phi K^*$, where ϕ and K^* go subsequently into $K\bar{K}$ and $K\pi$ pairs, respectively. Following the definition given in Ref. [15], the external momenta of the decay chain will be denoted as p, q for the two meson pairs, and $p_{1,2}^{(\prime)}$ for the four final-state mesons, with the specific charge assignment according to

$$B(p_B) \to \phi(q)K^*(p) \to K(p_2)\bar{K}(p_2')K(p_1)\pi(p_1'), \tag{3}$$

where $p_B = p + q$, $p = p_1 + p_1'$, and $q = p_2 + p_2'$, which obey the momentum conservation. For simplicity, we shall work in the rest frame of the B meson in the light-cone coordinates such that $p_B = \frac{M}{\sqrt{2}}(1, 1, \mathbf{0}_T)$ with the B meson mass M. The momenta of ϕ and K^* can be written as

$$q = \frac{M}{\sqrt{2}}(f^-, f^+, \mathbf{0}_T), \qquad p = \frac{M}{\sqrt{2}}(g^+, g^-, \mathbf{0}_T), \tag{4}$$

respectively. The factors $g^\pm$ and $f^\pm$ are related to the invariant masses of the meson pairs via $p^2 = \omega_1^2$ and $q^2 = \omega_2^2$, which can be written as

$$\begin{aligned} g^\pm &= \frac{1}{2}\left[1 + \eta_1 - \eta_2 \pm \sqrt{(1 + \eta_1 - \eta_2)^2 - 4\eta_1}\right], \\ f^\pm &= \frac{1}{2}\left[1 - \eta_1 + \eta_2 \pm \sqrt{(1 + \eta_1 - \eta_2)^2 - 4\eta_1}\right], \end{aligned} \tag{5}$$

with the mass ratios $\eta_{1,2} = \omega_{1,2}^2/M^2$. For the meson pairs in the P-wave configurations, the corresponding longitudinal polarization vectors are defined as

$$\epsilon_q = \frac{1}{\sqrt{2\eta_2}}(-f^-, f^+, \mathbf{0}_T), \quad \epsilon_p = \frac{1}{\sqrt{2\eta_1}}(g^+, -g^-, \mathbf{0}_T), \tag{6}$$

which satisfy the normalization $\epsilon_q^2 = \epsilon_p^2 = -1$ and the orthogonality $\epsilon_q \cdot q = \epsilon_p \cdot p = 0$.

Introducing the meson momentum fraction ζ for each meson pair, the individual momenta of the four final states can be expressed as

$$\begin{aligned}
p_1 &= \left(\frac{M}{\sqrt{2}}\left(\zeta_1 + \frac{r_1 - r_1'}{2\eta_1}\right)g^+, \frac{M}{\sqrt{2}}\left(1 - \zeta_1 + \frac{r_1 - r_1'}{2\eta_1}\right)g^-, \mathbf{p}_T\right),\\
p_1' &= \left(\frac{M}{\sqrt{2}}\left(1 - \zeta_1 - \frac{r_1 - r_1'}{2\eta_1}\right)g^+, \frac{M}{\sqrt{2}}\left(\zeta_1 - \frac{r_1 - r_1'}{2\eta_1}\right)g^-, -\mathbf{p}_T\right),\\
p_2 &= \left(\frac{M}{\sqrt{2}}\left(1 - \zeta_2 + \frac{r_2 - r_2'}{2\eta_2}\right)f^-, \frac{M}{\sqrt{2}}\left(\zeta_2 + \frac{r_2 - r_2'}{2\eta_2}\right)f^+, \mathbf{q}_T\right),\\
p_2' &= \left(\frac{M}{\sqrt{2}}\left(\zeta_2 - \frac{r_2 - r_2'}{2\eta_2}\right)f^-, \frac{M}{\sqrt{2}}\left(1 - \zeta_2 - \frac{r_2 - r_2'}{2\eta_2}\right)f^+, -\mathbf{q}_T\right),
\end{aligned} \tag{7}$$

with the mass ratios $r_i^{(\prime)} = m_i^{(\prime)2}/M^2$ $(i = 1, 2)$, where $m_i^{(\prime)}$ is the mass of the meson $P_i^{(\prime)}$. The transverse momenta $\mathbf{p}_T$ and $\mathbf{q}_T$ can be derived from the on-shell condition $p_i^{(\prime)2} = m_i^{(\prime)2}$ for each final-state meson, which yields

$$|\mathbf{p}_T|^2 = \omega_1^2[\zeta_1(1-\zeta_1) + \alpha_1], \quad |\mathbf{q}_T|^2 = \omega_2^2[\zeta_2(1-\zeta_2) + \alpha_2], \tag{8}$$

with the factors

$$\alpha_i = \frac{(r_i - r_i')^2}{4\eta_i^2} - \frac{r_i + r_i'}{2\eta_i}. \tag{9}$$

Comparing Eqs. (4) and (7), we find the meson momentum fractions modified by the meson masses,

$$\frac{p_1^+}{p^+} = \zeta_1 + \frac{r_1 - r_1'}{2\eta_1}, \qquad \frac{p_2^-}{q^-} = \zeta_2 + \frac{r_2 - r_2'}{2\eta_2}. \tag{10}$$

It is easy to derive the relation between ζ and the polar angles θ in Fig. 1 in the meson-pair rest frame:

$$2\zeta_i - 1 = \sqrt{1 + 4\alpha_i}\cos\theta_i, \tag{11}$$

with the bound

$$\zeta_i \in \left[\frac{1 - \sqrt{1+4\alpha_i}}{2}, \frac{1 + \sqrt{1+4\alpha_i}}{2}\right]. \tag{12}$$

Note that Eq. (11) reduces to the conventional form in Refs. [68,69] in the limit of massless.

The Feynman diagrams for the hard kernels associated with the considered four-body B meson decays are displayed in Fig. 2, each of which contains a single hard gluon exchange at leading order in the PQCD approach. The first row represents the emission type, while the second row represents the annihilation one. Each type is further classified as factorizable, in which a gluon attaches to quarks in the same meson, and nonfactorizable, in which a gluon attaches to quarks in distinct mesons. For the evaluation of the hard kernels, we define three valence quark momenta labeled by k_B, k_1, and k_2 in Fig. 2(a) as

$$\begin{aligned}
k_B &= (0, x_B p_B^-, \mathbf{k}_{BT}), \qquad k_1 = (x_1 p^+, 0, \mathbf{k}_{1T}),\\
k_2 &= (0, x_2 q^-, \mathbf{k}_{2T}),
\end{aligned} \tag{13}$$

with the parton momentum fractions x_i, and the parton transverse momenta k_{iT}. Since k_1 and k_2 move with the corresponding meson pair in the plus and minus direction, respectively, the minus (plus) component of $k_1(k_2)$ can be neglected due to its small size. We also drop k_B^+ because it does not appear in the hard kernels for dominant factorizable contributions.

C. Two-meson distribution amplitudes

The light-cone matrix elements for S-wave $K\bar{K}$ and $K\pi$ can be decomposed, up to twist 3, into [17,27]

$$\begin{aligned}
\Phi_{(K\bar{K})_S}(x_2, \omega_2) &= \frac{1}{\sqrt{2N_c}}[\not{\phi}\phi^0_{(K\bar{K})_S}(x_2, \omega_2) + \omega_2\phi^s_{(K\bar{K})_S}(x_2, \omega_2) + \omega_2(\not{v}\not{n} - 1)\phi^t_{(K\bar{K})_S}(x_2, \omega_2)],\\
\Phi_{(K\pi)_S}(x_1, \omega_1) &= \frac{1}{\sqrt{2N_c}}[\not{p}\phi^0_{(K\pi)_S}(x_1, \omega_1) + \omega_1\phi^s_{(K\pi)_S}(x_1, \omega_1) + \omega_1(\not{n}\not{v} - 1)\phi^t_{(K\pi)_S}(x_1, \omega_1)],
\end{aligned} \tag{14}$$

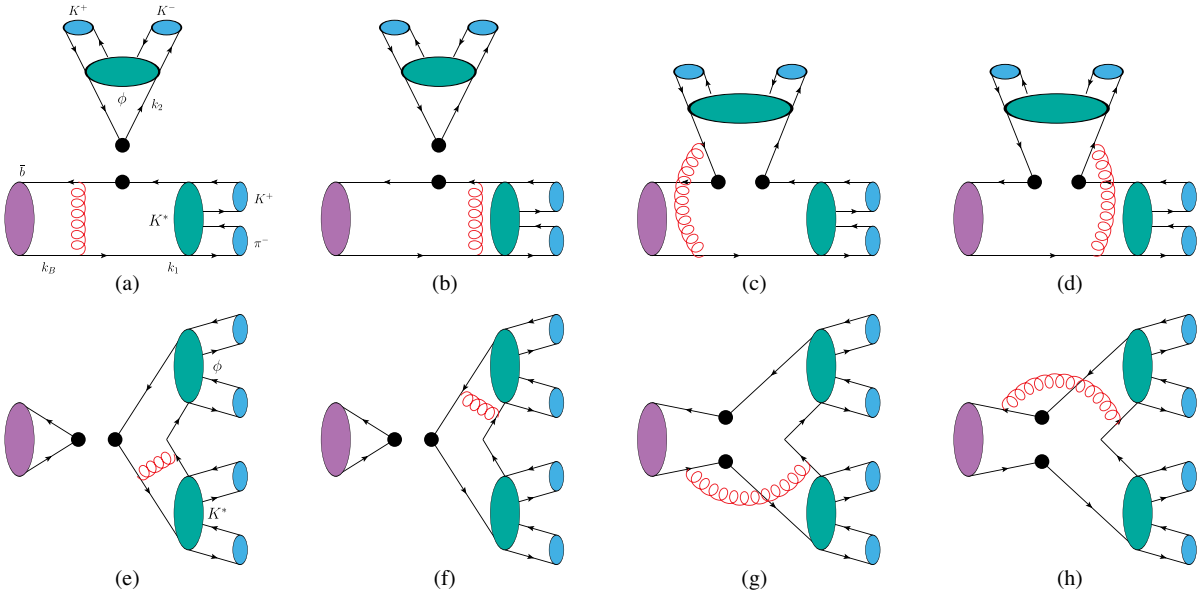

FIG. 2. Leading-order diagrams for the $B \to \phi(\to K\bar{K})K^*(\to K\pi)$ decays, where the symbol black circle denotes a weak vertex. The first (second) row correspond to the emission (annihilation) type diagrams, which are further classified into the factorizable ones (a), (b), ((e), (f)), and the nonfactorizable ones (c), (d), ((g), (h)).

where $n = (1, 0, \mathbf{0}_T)$ and $v = (0, 1, \mathbf{0}_T)$ are two dimensionless vectors. The parametrization of various twists DAs take the forms

$$\phi^0_{(PP')_S}(x,\omega) = \begin{cases} \frac{9F_{(PP')_S}(\omega)}{\sqrt{2N_c}} a_{PP'} x(1-x)(1-2x), & PP' = K\bar{K}, \\ \frac{3F_{(PP')_S}(\omega)}{\sqrt{2N_c}} x(1-x)\left[\frac{1}{\mu_S} + B_1 3(1-2x) + B_3 \frac{5}{2}(1-2x)(7(1-2x)^2-3)\right], & PP' = K\pi, \end{cases}$$
$$\phi^s_{(PP')_S}(x,\omega) = \frac{F_{(PP')_S}(\omega)}{2\sqrt{2N_c}},$$
$$\phi^t_{(PP')_S}(x,\omega) = \frac{F_{(PP')_S}(\omega)}{2\sqrt{2N_c}}(1-2x), \tag{15}$$

with the ratio $\mu_S = \omega_1/(m_s - m_q)$, where $m_s(1\ \text{GeV}) = 119$ MeV [70,71] is the running strange quark mass and the light quark masses m_q, $q = u, d$, are set to zero. The values of the Gegenbauer moments for the twist-2 DAs are taken as [66,70–72]

$$a_{K\bar{K}} = 0.80 \pm 0.16, \qquad B_1 = -0.57 \pm 0.13,$$
$$B_3 = -0.42 \pm 0.22. \tag{16}$$

Because the available data are not yet precise enough to extract more Gegenbauer moments, the two twist-3 DAs are chosen as asymptotic forms.

For the scalar form factor $F_{(K\pi)_S}$, we follow the LASS line shape [73], which includes an effective-range nonresonant component with the $K_0^*(1430)$ resonance Breit-Wigner tail. The explicit expression is given by

$$F_{(K\pi)_S}(\omega) = \frac{\omega}{k(\omega)} \cdot \frac{1}{\cot\delta_B - i} + e^{2i\delta_B} \frac{m_0^2 \Gamma_0 / k(m_0)}{m_0^2 - \omega^2 - i m_0^2 \frac{\Gamma_0}{\omega}\frac{k(\omega)}{k(m_0)}},$$
$$\cot\delta_B = \frac{1}{ak(\omega)} + \frac{1}{2} b k(\omega), \tag{17}$$

where m_0 (Γ_0) is the mass (width) of $K_0^*(1430)$. The kaon three-momentum $k(\omega)$ is written, in the $K\pi$ center-of-mass frame, as

$$k(\omega) = \frac{\sqrt{[\omega^2 - (m_K + m_\pi)^2][\omega^2 - (m_K - m_\pi)^2]}}{2\omega}, \tag{18}$$

with $m_{K(\pi)}$ the known kaon (pion) mass, and $k(m_0)$ being the same quantity evaluated at the nominal resonance mass m_0. We use the following values for the resonance mass, width, scattering length, and effective-range parameters: $m_0 = 1450 \pm 80$ MeV, $\Gamma_0 = 400 \pm 230$ MeV, $a = 3.2 \pm 1.8\ \text{GeV}^{-1}$, and $b = 0.9 \pm 1.1\ \text{GeV}^{-1}$ [15,74].

For the scalar form factor of the $K\bar{K}$ system, the main resonance is $f_0(980)$ in the concerned mass window, since its mass is very close to the $K\bar{K}$ threshold, which can strongly influence the resonance shape. We follow Ref. [66] to take the widely accepted prescription proposed by Flatté [75]

$$F_{(K\bar{K})_S}(\omega)=\frac{m^2_{f_0(980)}}{m^2_{f_0(980)}-\omega^2-im_{f_0(980)}(g_{\pi\pi}\rho_{\pi\pi}+g_{KK}\rho_{KK}F^2_{KK})} \tag{19}$$

with $m_{f_0(980)}=939\ \mathrm{MeV}/c^2, g_{\pi\pi}=199\ \mathrm{MeV}/c^2, g_{KK}=3g_{\pi\pi}$ [58]. The exponential term $F_{KK}=e^{-\alpha q_K^2}$ is introduced above the $K\bar{K}$ threshold to reduce the ρ_{KK} factor as ω increases, where q_k is the momentum of the kaon in the $K\bar{K}$ rest frame and $\alpha=2.0\pm0.25\ \mathrm{GeV}^{-2}$ [76,77].

In Ref. [15] we have updated the P-wave DAs including both longitudinal and transverse polarizations for the $K\pi$ pair, whose explicit expressions read

$$\begin{aligned}
\Phi^L_{(K\pi)_P}(x_1,\zeta_1,\omega_1)&=\frac{1}{\sqrt{2N_c}}\left[\omega_1\not{\epsilon}_p\phi^0_{(K\pi)_P}(x_1,\omega_1)+\omega_1\phi^s_{(K\pi)_P}(x_1,\omega_1)+\frac{\not{p}_1\not{n}_1'-\not{n}_1'\not{p}_1}{\omega_1(2\zeta_1-1)}\phi^t_{(K\pi)_P}(x_1,\omega_1)\right](2\zeta_1-1),\\
\Phi^T_{(K\pi)_P}(x_1,\zeta_1,\omega_1)&=\frac{1}{\sqrt{2N_c}}\left[\gamma_5\not{\epsilon}_T\not{p}\phi^T_{(K\pi)_P}(x_1,\omega_1)+\omega_1\gamma_5\not{\epsilon}_T\phi^a_{(K\pi)_P}(x_1,\omega_1)+i\omega_1\frac{\epsilon^{\mu\nu\rho\sigma}\gamma_\mu\epsilon_{T\nu}p_\rho n_{-\sigma}}{p\cdot n_-}\phi^v_{(K\pi)_P}(x_1,\omega_1)\right]\\
&\quad\sqrt{\zeta_1(1-\zeta_1)+\alpha_1},
\end{aligned} \tag{20}$$

respectively. Naively, the P-wave $K\bar{K}$ ones can be obtained with the following replacement:

$$x_1\to x_2,\qquad \omega_1\to\omega_2,\qquad \zeta_1\to\zeta_2,\qquad \alpha_1\to\alpha_2,\qquad p\to q,\qquad \epsilon_p\to\epsilon_q,\qquad p_1^{(\prime)}\to p_2^{(\prime)}. \tag{21}$$

The various twist DAs for the P-wave $K\bar{K}$ and $K\pi$ systems are parametrized as [67]

$$\begin{aligned}
\phi^0_{K\bar{K}}(x_2,\omega_2)&=\frac{3}{\sqrt{2N_c}}F^{\parallel}_{K\bar{K}}(\omega_2)x_2(1-x_2)[1+a^0_{2\phi}C^{3/2}_2(2x_2-1)],\\
\phi^s_{K\bar{K}}(x_2,\omega_2)&=\frac{3}{2\sqrt{2N_c}}F^{\perp}_{K\bar{K}}(\omega_2)(1-2x_2),\\
\phi^t_{K\bar{K}}(x_2,\omega_2)&=\frac{3}{2\sqrt{2N_c}}F^{\perp}_{K\bar{K}}(\omega_2)(1-2x_2)^2,\\
\phi^T_{K\bar{K}}(x_2,\omega_2)&=\frac{3}{\sqrt{2N_c}}F^{\perp}_{K\bar{K}}(\omega_2)x_2(1-x_2)[1+a^0_{2\phi}C^{3/2}_2(2x_2-1)],\\
\phi^a_{K\bar{K}}(x_2,\omega_2)&=\frac{3}{4\sqrt{2N_c}}F^{\parallel}_{K\bar{K}}(\omega_2)(1-2x_2),\\
\phi^v_{K\bar{K}}(x_2,\omega_2)&=\frac{3}{8\sqrt{2N_c}}F^{\parallel}_{K\bar{K}}(\omega_2)[1+(1-2x_2)^2],\\
\phi^0_{K\pi}(x_1,\omega_1)&=\frac{3}{\sqrt{2N_c}}F^{\parallel}_{K\pi}(\omega_1)x_1(1-x_1)[1+a^0_{1K^*}C^{3/2}_1(2x_1-1)+a^0_{2K^*}C^{3/2}_2(2x_1-1)],\\
\phi^s_{K\pi}(x_1,\omega_1)&=\frac{3}{2\sqrt{2N_c}}F^{\perp}_{K\pi}(\omega_1)(1-2x_1),\\
\phi^t_{K\pi}(x_1,\omega_1)&=\frac{3}{2\sqrt{2N_c}}F^{\perp}_{K\pi}(\omega_1)(1-2x_1)^2,\\
\phi^T_{K\pi}(x_1,\omega_1)&=\frac{3}{\sqrt{2N_c}}F^{\perp}_{K\pi}(\omega_1)x_1(1-x_1)[1+a^0_{1K^*}C^{3/2}_1(2x_1-1)+a^0_{2K^*}C^{3/2}_2(2x_1-1)],\\
\phi^a_{K\pi}(x_1,\omega_1)&=\frac{3}{4\sqrt{2N_c}}F^{\parallel}_{K\pi}(\omega_1)(1-2x_1),\\
\phi^v_{K\pi}(x_1,\omega_1)&=\frac{3}{8\sqrt{2N_c}}F^{\parallel}_{K\pi}(\omega_1)[1+(1-2x_1)^2],
\end{aligned} \tag{22}$$

with the Gegenbauer polynomials

$$C_1^{3/2}(t) = 3t, \qquad C_2^{3/2}(t) = \frac{3}{2}(5t^2 - 1). \tag{23}$$

The values of the Gegenbauer moments associated with longitudinal polarization are adopted as

$$a^0_{1K^*} = 0.31 \pm 0.16, \qquad a^0_{2K^*} = 1.19 \pm 0.10,$$
$$a^0_{2\phi} = -0.31 \pm 0.19, \tag{24}$$

which are determined from a global analysis in the PQCD approach [67]. We do not distinguish the Gegenbauer moments for the longitudinal and transverse polarizations in our numerical calculations due to a lack of rigorous theoretical and experimental information on the transverse polarizations.

Since the $K\pi$ spectrum is dominated by the vector $K^*(892)$ resonance in the selected invariant mass range, the P-wave timelike form factor $F^{\parallel}_{K\pi}$ is parametrized as the relativistic Breit-Wigner model [78,79]

$$F^{\parallel}_{K\pi}(\omega) = \frac{m^2_{K^*}}{m^2_{K^*} - \omega^2 - i m_{K^*}\Gamma(\omega)}, \tag{25}$$

where $m_{K^*} = 895.81$ MeV is the $K^*(892)$ mass. The mass-dependent width is given by

$$\Gamma(\omega) = \Gamma_{K^*}\frac{k^3(\omega)}{k^3(m_{K^*})}\frac{m_{K^*}}{\omega}\frac{1 + r^2k^2(m_{K^*})}{1 + r^2k^2(\omega)}, \tag{26}$$

where $\Gamma_{K^*} = 47.4$ MeV is the natural width of the $K^*(892)$ meson and $r = 3.4$ GeV^{-1} is the interaction radius [58]. The P-wave $K\bar{K}$ one, denoted $F^{\parallel}_{K\bar{K}}$, is modeled in a similar way using the values $m_\phi = 1019.455$ MeV and $\Gamma_\phi = 4.26$ MeV [58]. For another form factor $F^{\perp}$, we assume the approximate relation $F^{\perp}/F^{\parallel} \sim f_V^T/f_V$ with $f_V^{(T)}$ being the tensor (vector) decay constant of the vector resonance.

III. NUMERICAL RESULTS

In this section we discuss in detail some physical observables, such as branching ratios, S-wave fractions, polarization fractions, direct CP asymmetries, and TPAs, for the concerned decays. The related input parameters for the numerical calculations are collected in Table II. The decay constants used the values from Refs. [15,60,67], while the meson masses, Wolfenstein parameters, and the lifetimes are taken from the PDG review [37]. We neglect uncertainties on the constants since they are negligible with respect to other sources of uncertainty. The parameters relevant to the $K\bar{K}$ and $K\pi$ DAs have been specified in the previous section.

Another key input in the PQCD calculations is the B meson distribution amplitude. We adopt the conventional form from Refs. [80,81] of the leading Lorentz structure

$$\phi_B(x,b) = N_B x^2(1-x)^2 \exp\left[-\frac{x^2M^2}{2\omega_b^2} - \frac{\omega_b^2 b^2}{2}\right], \tag{27}$$

with the shape parameter $\omega_b = 0.40$ GeV for $B_{u,d}$ mesons and $\omega_b = 0.48$ GeV for a B_s meson [82]. The normalization constant N_B is related to the decay constant f_B via the normalization

$$\int_0^1 \phi_B(x, b=0)dx = \frac{f_B}{2\sqrt{2N_c}}. \tag{28}$$

For more alternative models of the B meson DA and the subleading contributions, one can refer to Refs. [83–87].

A. *CP* averaged four-body branching ratios and *S*-wave fractions

The phase space of a four-body decay relies on the five kinematic variables, that is, three helicity angles shown in Fig. 1 and two invariant masses. In the B meson rest frame, the fivefold differential decay rate can be written as

$$\frac{d^5\Gamma}{d\theta_1 d\theta_2 d\varphi d\omega_1 d\omega_2} = \frac{k(\omega_1)k(\omega_2)k(\omega_1,\omega_2)}{16(2\pi)^6M^2}|A|^2, \tag{29}$$

where $k(\omega_1,\omega_2) = \sqrt{[M^2-(\omega_1+\omega_2)^2][M^2-(\omega_1-\omega_2)^2]}/(2M)$ is the magnitude of the three-momentum of the meson pair in the B meson rest frame. By appropriate variable changes, Eq. (29) is equivalent to the one in Ref. [88]. Replacing the helicity angles θ_i by the meson momentum fractions ζ_i via Eq. (11) and integrating the decay rate with respect to all independent variables, we obtain

TABLE II. The decay constants are taken from Refs. [15,60,67]. Other parameters are from PDG 2020 [37].

Mass (GeV)	$M_{B_s} = 5.37$		$M_B = 5.28$	$m_K = 0.494$		$m_\pi = 0.14$
Wolfenstein parameters	$\lambda = 0.22650$		$A = 0.790$	$\bar{\rho} = 0.141$		$\bar{\eta} = 0.357$
Decay constants (GeV)	$f_{B_s} = 0.24$	$f_B = 0.21$	$f_{\phi(1020)} = 0.215$	$f^T_{\phi(1020)} = 0.186$	$f_{K^*} = 0.217$	$f^T_{K^*} = 0.185$
Lifetime (ps)	$\tau_{B_s} = 1.51$			$\tau_{B^0} = 1.52$		$\tau_{B^+} = 1.638$

$$\Gamma = \frac{1}{4(2\pi)^6 M^2 \sqrt{1+4\alpha_1}\sqrt{1+4\alpha_2}} \int k(\omega_1)k(\omega_2)k(\omega_1,\omega_2)|A|^2 d\zeta_1 d\zeta_2 d\varphi d\omega_1 d\omega_2, \tag{30}$$

where the selected invariant mass ranges for the $K\bar{K}$ and $K\pi$ pairs are $m_\phi - 0.015 < \omega_2 < m_\phi + 0.015$ (GeV) and $m_{K^*} - 0.15 < \omega_1 < m_{K^*} + 0.15$ (GeV), respectively. The total amplitude (A) can be decomposed into six helicity components shown in Table I with different ζ_i and φ dependencies [15]

$$\begin{aligned} A = {} & \frac{2\zeta_1 - 1}{\sqrt{1+4\alpha_1}} \frac{2\zeta_2 - 1}{\sqrt{1+4\alpha_2}} A_0 + 2\sqrt{2} \sqrt{\frac{\zeta_1(1-\zeta_1)+\alpha_1}{1+4\alpha_1}} \sqrt{\frac{\zeta_2(1-\zeta_2)+\alpha_2}{1+4\alpha_2}} \cos(\varphi) A_\parallel \\ & + i2\sqrt{2} \sqrt{\frac{\zeta_1(1-\zeta_1)+\alpha_1}{1+4\alpha_1}} \sqrt{\frac{\zeta_2(1-\zeta_2)+\alpha_2}{1+4\alpha_2}} \sin(\varphi) A_\perp + \frac{2\zeta_1 - 1}{\sqrt{1+4\alpha_1}} A_{VS} + \frac{2\zeta_2 - 1}{\sqrt{1+4\alpha_2}} A_{SV} + A_{SS}. \end{aligned} \tag{31}$$

The branching ratio of each component is then

$$\mathcal{B}_h = \frac{\tau_B}{4(2\pi)^6 M^2} \frac{2\pi}{9} Y_h \int d\omega_1 d\omega_2 k(\omega_1) k(\omega_2) k(\omega_1,\omega_2) |A_h|^2, \tag{32}$$

with

$$Y_h = \begin{cases} 1, & h = 0, \parallel, \perp \\ 3, & h = SV, VS \\ 9, & h = SS, \end{cases} \tag{33}$$

which come from the integrations over $\zeta_1, \zeta_2, \varphi$. Combining Eq. (32) with its counterpart of the corresponding CP-conjugated process, we can derive the CP-averaged branching ratio of each component and their sum

$$\mathcal{B}_h^{\text{avg}} = \frac{1}{2}(\bar{\mathcal{B}}_h + \mathcal{B}_h), \qquad \mathcal{B}_{\text{total}} = \sum_h \mathcal{B}_h, \tag{34}$$

with h running over the six helicities as stated above.

The numerical results are summarized in Table III, where the first quoted uncertainty is due to the shape parameters ω_b in the $B_{(s)}$ meson DAs with 10% variation, the second uncertainty is caused by the variation of the Gegenbauer moments in the two-meson DAs shown in Eqs. (16) and (24), and the last one comes from the hard scale t that varies from $0.75t$ to $1.25t$ and the QCD scale $\Lambda_{\text{QCD}} = 0.25 \pm 0.05$ GeV. The three uncertainties are comparable, and their combined impacts could exceed 50%, implying that the nonperturbative parameters in the DAs of the initial and final states must be more precisely restricted, and the higher-order correction to four-body B meson decays is critical. The concerned three channels are all penguin-dominated decays. The B^0 and B^+ modes involve the $b \to s$ transition and therefore have relatively large branching ratios of $\mathcal{O}(10^{-7}$–$10^{-6})$, while the B_s channels, mediated by the $b \to d$ transition, are generally 1 or 2 orders of magnitudes smaller.

Although the P-wave contributions dominate in the selected mass regions, the S-wave contributions, which are strongly sensitive to the integrating ranges, cannot be neglected. In order to compare the relative size of the S-wave contributions, one can define the S-wave fractions as

$$f_\sigma = \frac{\mathcal{B}_\sigma}{\mathcal{B}_{\text{total}}}, \tag{35}$$

with $\sigma = \{SS, SV, VS\}$, and the total S-wave fraction as $f_{\text{S-wave}} = f_{SS} + f_{SV} + f_{VS}$. Using the PQCD predictions

TABLE III. PQCD predictions for the CP-averaged branching ratios of various components and their sum in the $B_{(s)} \to (K\bar{K})(K\pi)$ decays within the $K\bar{K}(K\pi)$ invariant mass window of 15 (150) MeV around the $\phi(K^*(982))$ resonance.

Components	$B^0 \to (K^+K^-)(K^+\pi^-)$	$B_s^0 \to (K^+K^-)(K^-\pi^+)$	$B^+ \to (K^+K^-)(K^0\pi^+)$
$\mathcal{B}_0$	$1.8^{+0.7+0.3+0.6}_{-0.6-0.4-0.4} \times 10^{-6}$	$3.1^{+1.2+1.0+1.6}_{-0.8-0.9-1.2} \times 10^{-8}$	$1.8^{+0.9+0.4+0.7}_{-0.5-0.3-0.4} \times 10^{-6}$
$\mathcal{B}_\parallel$	$3.1^{+0.5+0.4+1.3}_{-0.4-0.4-0.8} \times 10^{-7}$	$5.3^{+0.6+2.0+2.5}_{-0.3-1.4-1.3} \times 10^{-9}$	$3.4^{+0.6+0.5+1.3}_{-0.4-0.4-0.8} \times 10^{-7}$
$\mathcal{B}_\perp$	$3.3^{+0.6+0.5+1.3}_{-0.4-0.4-0.8} \times 10^{-7}$	$5.2^{+0.3+1.9+2.6}_{-0.3-1.6-1.5} \times 10^{-9}$	$3.6^{+0.6+0.4+1.3}_{-0.5-0.5-0.9} \times 10^{-7}$
$\mathcal{B}_{SS}$	$4.7^{+2.0+2.4+1.8}_{-1.4-1.9-1.4} \times 10^{-8}$	$1.3^{+0.7+0.6+0.5}_{-0.5-0.5-0.4} \times 10^{-9}$	$5.2^{+2.1+2.6+2.0}_{-1.5-2.1-1.6} \times 10^{-8}$
$\mathcal{B}_{VS}$	$4.6^{+1.2+1.0+1.7}_{-0.9-1.0-1.4} \times 10^{-7}$	$5.0^{+2.3+1.2+2.7}_{-1.8-1.1-2.1} \times 10^{-9}$	$4.8^{+1.5+1.0+1.8}_{-1.1-1.0-1.3} \times 10^{-7}$
$\mathcal{B}_{SV}$	$2.2^{+0.6+0.4+0.8}_{-0.5-0.4-0.6} \times 10^{-7}$	$1.6^{+0.5+0.8+0.5}_{-0.4-0.6-0.4} \times 10^{-9}$	$2.5^{+0.7+0.5+0.9}_{-0.5-0.4-0.7} \times 10^{-7}$
$\mathcal{B}_{\text{total}}$	$3.2^{+1.0+0.4+1.1}_{-0.9-0.5-0.8} \times 10^{-6}$	$4.9^{+1.6+1.4+2.4}_{-1.1-1.2-1.6} \times 10^{-8}$	$3.3^{+1.2+0.6+1.2}_{-0.8-0.5-0.8} \times 10^{-6}$

TABLE IV. S-wave fractions in the $B_{(s)} \to (K\bar{K})(K\pi)$ decays within the $K\bar{K}(K\pi)$ invariant mass window of 15 (150) MeV around the $\phi(K^*(982))$ resonance. The data are taken from Ref. [58], where the first uncertainty is statistical and the second is systematic.

Modes	f_{SS}	f_{VS}	f_{SV}	$f_{S\text{-wave}}$
$B^0 \to (K^+K^-)(K^+\pi^-)$	$0.015^{+0.001+0.007+0.002}_{-0.000-0.006-0.002}$	$0.144^{+0.013+0.022+0.016}_{-0.007-0.020-0.015}$	$0.069^{+0.006+0.014+0.002}_{-0.002-0.011-0.005}$	$0.228^{+0.020+0.037+0.018}_{-0.009-0.032-0.022}$
LHCb [58]	⋯	$0.143 \pm 0.013 \pm 0.012$	$0.122 \pm 0.013 \pm 0.008$	⋯
$B_s^0 \to (K^+K^-)(K^-\pi^+)$	$0.027^{+0.004+0.013+0.002}_{-0.004-0.011-0.002}$	$0.102^{+0.010+0.032+0.022}_{-0.018-0.030-0.029}$	$0.033^{+0.000+0.016+0.004}_{-0.001-0.014-0.007}$	$0.162^{+0.014+0.057+0.027}_{-0.023-0.050-0.037}$
$B^+ \to (K^+K^-)(K^0\pi^+)$	$0.016^{+0.000+0.008+0.001}_{-0.001-0.006-0.002}$	$0.146^{+0.003+0.021+0.014}_{-0.006-0.021-0.009}$	$0.076^{+0.003+0.014+0.001}_{-0.005-0.013-0.007}$	$0.238^{+0.006+0.035+0.015}_{-0.012-0.035-0.018}$

as given in Table III, it is straightforward to obtain the numerical results of S-wave fractions in each channel as exhibited in Table IV.

The predicted two single S-wave fractions for the B^0 mode are well consistent with the data from Ref. [58]. In Ref. [58], it is assumed that the double S-wave component is negligible. In our calculations, as can be seen in Table IV, the double S-wave fractions of all the three modes are estimated to be less than 3% and can be safely ignored. Therefore the assumption in [58] is reasonable in the selected invariant mass ranges. However, we will discuss later that the S-wave contributions will be enhanced rapidly with increasing invariant mass ranges. The predicted total S-wave fraction for the B_s mode is in agreement with the LHCb data 0.16 ± 0.02 [59] obtained from the total ϕK^{*0} purity by combining the K^+K^- and $K^+\pi^-$ contributions. It is assumed in Ref. [59] that the S-wave component is the same for $B^0 \to \phi K^{*0}$ and $B_s^0 \to \phi \bar{K}^{*0}$ decays, so that the larger sample of $B^0 \to \phi K^{*0}$ decays can be used. This assumption lead to a large systematic uncertainty of this measurement, which is expected to scale with larger data samples in future. From Table IV, the total S-wave contributions could be as large as 20% of the total decay rate, indicating they are numerically significant in the given mass regions.

The S-wave channels were also measured by other collaborations with a different $K\pi$ mass range. The branching ratio for $B^0 \to \phi(K\pi)_0^*$ mode was measured to be $(4.3 \pm 0.4(\text{stat}) \pm 0.4(\text{syst})) \times 10^{-6}$ by the Belle experiment [35], which was consistent with the previous *BABAR* measurement, $(4.3 \pm 0.6(\text{stat}) \pm 0.4(\text{syst})) \times 10^{-6}$ [32]. We note that the above two measurements were performed in a broad $K\pi$ invariant mass range $0.7 < m_{K\pi} < 1.55$ GeV. For comparison, we derive the single S-wave branching ratio with the same mass region,

$$\mathcal{B}(B^0 \to \phi(\to K^+K^-)(K\pi)_0^*(\to K^+\pi^-)) = (1.2^{+0.4+0.3+0.5}_{-0.1-0.2-0.3}) \times 10^{-6}, \tag{36}$$

which is more than twice the number in Table III. After correcting for the secondary branching fraction $\mathcal{B}(\phi \to K^+K^-) = 0.5$ and $\mathcal{B}((K\pi)_0^* \to K^+\pi^-) = 2/3$, one can obtain the two-body decay branching ratio in the narrow-width limit,

$$\mathcal{B}(B^0 \to \phi(K\pi)_0^*) = (3.6^{+1.2+0.9+1.5}_{-0.3-0.6-0.9}) \times 10^{-6}, \tag{37}$$

which complies with the above two measurements and the previous two-body PQCD value of $(3.7^{+0.8+0.1+3.7}_{-0.7-0.1-1.7}) \times 10^{-6}$ for the S1 scenario [89].

In Ref. [90], the *BABAR* Collaboration measured the $B^0 \to f_0(980)K^{*0}(892)$ and $B^0 \to f_0(980)(K\pi)_0^*$ decays, where $f_0(980)$ was reconstructed through $f_0(980) \to \pi\pi$ within the $\pi\pi$ invariant mass range $0.47 < m_{\pi\pi} < 1.07$ GeV. For the $K\pi$ mass spectrum, the two channels were analyzed separately. The former was performed in the "low mass region," $0.75 < m_{K\pi} < 1.0$ GeV, while the latter was performed in the "high mass region," $1.0 < m_{K\pi} < 1.55$ GeV. The quoted branching ratios yield [90]

$$\begin{aligned}\mathcal{B}(B^0 \to f_0(980)(K\pi)_0^*) \times \mathcal{B}(f_0(980) \to \pi\pi) \times \mathcal{B}((K\pi)_0^* \to K\pi) &= (3.1 \pm 0.8 \pm 0.7) \times 10^{-6}, \\ \mathcal{B}(B^0 \to f_0(980)K^{*0}(892)) \times \mathcal{B}(f_0(980) \to \pi\pi) &= (5.7 \pm 0.6 \pm 0.4) \times 10^{-6},\end{aligned} \tag{38}$$

where the uncertainties are statistical and systematic, respectively. The Belle Collaboration presented a smaller value of $\mathcal{B}(B^0 \to f_0(980)K^{*0}(892)) = (1.4^{+0.6+0.6}_{-0.5-0.4}) \times 10^{-6}$, obtained for $m_{K\pi} \in (0.75, 1.2)$ GeV and $m_{\pi\pi} \in (0.55, 1.2)$ GeV, with 2.5σ significance [91]. For comparison we recalculate the four-body branching ratios for the scalar-scalar and scalar-vector modes with the same $K\pi$ mass region as the *BABAR* experiment. In the narrow-width limit, we obtain the products

$$\begin{aligned}\mathcal{B}(B^0 \to f_0(980)(K\pi)_0^*)) \times \mathcal{B}(f_0(980) \to K^+K^-) \times \mathcal{B}((K\pi)_0^* \to K^+\pi^-) &= (2.1^{+0.7+0.9+0.9}_{-0.6-0.7-0.6}) \times 10^{-7}, \\ \mathcal{B}(B^0 \to f_0(980)K^{*0}(892)) \times \mathcal{B}(f_0(980) \to K^+K^-) \times \mathcal{B}(K^{*0}(892) \to K^+\pi^-) &= (4.3^{+1.3+0.7+1.6}_{-0.9-0.7-1.2}) \times 10^{-7}.\end{aligned} \tag{39}$$

It is worth emphasizing that the above results cannot be directly compared with the data in Eq. (38) due to the absence of reliable information about $\mathcal{B}(f_0(980) \to K^+K^-)$ and $\mathcal{B}(f_0(980) \to \pi^+\pi^-)$. Assuming that the $f_0(980)$ resonance only couples to the $K\bar{K}$ and $\pi\pi$ channels and using the BES measurement [92]

$$\frac{\Gamma(f_0(980) \to \pi\pi)}{\Gamma(f_0(980) \to \pi\pi) + \Gamma(f_0(980) \to K\bar{K})} = 0.75^{+0.11}_{-0.13}, \quad (40)$$

and isospin relations $\Gamma(f_0(980) \to \pi^+\pi^-)/\Gamma(f_0(980) \to \pi\pi) = 2/3$ and $\Gamma(f_0(980) \to K^+K^-)/\Gamma(f_0(980) \to K\bar{K}) = 1/2$, we obtain the ratio

$$\frac{\Gamma(f_0(980) \to \pi^+\pi^-)}{\Gamma(f_0(980) \to K^+K^-)} = 4.0^{+0.6}_{-0.7}. \quad (41)$$

Plugging Eq. (41) into Eq. (39), and using above isospin relations, we estimate the branching ratio products in Eq. (38) to be $(1.9^{+1.4}_{-1.0}) \times 10^{-6}$ and $(3.9^{+2.0}_{-1.5}) \times 10^{-6}$, respectively, where the errors are added in quadrature. It can be seen that our prediction for the former is consistent with the *BABAR* value within uncertainties, but with central values that are somewhat lower. The number of the latter is in between *BABAR* and Belle measurements within errors. As pointed out in Refs. [93,94], the narrow-width approximation should be corrected by including finite-width effects for the broad scalar intermediate states. The results of Eq. (39), extracted from the four-body branching ratios, may suffer from a large uncertainty due to the finite-width effects of the scalar resonance. Thus the above comparisons is just a rough estimate for a cross-checking. In addition, we have shown that the S-wave contributions depend on the range of the $K\bar{K}$ and $K\pi$ invariant masses. In this study, the $K\bar{K}$ invariant mass is limited in a narrow window of ± 15 MeV around the known ϕ mass, and a broader integrated region would increase our results. It is expected that future experiments can directly reconstruct intermediate $f_0(980)$ resonance through $f_0(980) \to K^+K^-$ in the $B^0 \to (K^+K^-)(K^+\pi^-)$ decay.

B. Two-body branching ratios and polarization fractions

Since the width-to-mass ratio for ϕ and $K^*(892)$ is small, it is valid to apply the narrow width approximation for vector resonance to factorize the four-body process as three sequential two-body decays:

$$\mathcal{B}(B \to \phi(\to K\bar{K})K^*(\to K\pi)) \approx \mathcal{B}(B \to \phi K^*) \times \mathcal{B}(\phi \to K\bar{K}) \times \mathcal{B}(K^* \to K\pi), \quad (42)$$

for which we can extract the two-body $B \to \phi K^*$ branching ratios to compare with the current available predictions and experiments. The longitudinal, perpendicular, and parallel polarization fractions of the P-wave amplitudes are defined as

$$f_0 = \frac{\mathcal{B}_0}{\mathcal{B}_P}, \qquad f_\parallel = \frac{\mathcal{B}_\parallel}{\mathcal{B}_P}, \qquad f_\perp = \frac{\mathcal{B}_\perp}{\mathcal{B}_P}, \quad (43)$$

with $\mathcal{B}_P = \mathcal{B}_0 + \mathcal{B}_\parallel + \mathcal{B}_\perp$ being the total P-wave branching ratio. The numerical results together with other theoretical results from PQCD [52,60,62], QCDF [38,39,61,95], SCET [63] and FAT [64] are summarized in Table V for comparison. The world average values are taken from PDG [37] whenever available.

We see that the various approaches as well as experiment have similar branching ratios in magnitude for the B^0 and B^+ modes but quite different results for $\mathcal{B}(B_s^0 \to \phi\bar{K}^{*0})$. The predicted central values span a wide range: $(1.1 - 7.0) \times 10^{-7}$, which are generally below the current world average of $(1.14 \pm 0.30) \times 10^{-6}$. Our result is consistent with the recent QCDF calculation [95], and closer to the predictions from Refs. [38,61,62], but far from the previous PQCD value [60]. The discrepancy between theoretical predictions and experimental data remains an issue to be resolved.

According to the factorization assumption, the polarization fractions for the vector-vector modes should satisfy the naive counting rules [53]

$$f_0 \sim 1 - \mathcal{O}(m_V^2/M^2), \qquad f_\parallel \sim f_\perp \sim \mathcal{O}(m_V^2/M^2), \quad (44)$$

with m_V being the vector meson mass. The longitudinal polarization is naively expected to be $f_0 \sim 0.9$ in $B \to \phi K^*$ decays. However, a low longitudinal polarization of order 0.5 has been observed in the $B \to \phi K^*$ decays by Belle [34,35], *BABAR* [30–32], and LHCb [58,59], which indicates a significant departure from the naive expectation of predominant longitudinal polarization and poses an interesting challenge for theoretical interpretations. Several attempts to understand the values of within or beyond the standard model have been made [38–51,96–105].

In the PQCD approach, a large transverse polarization fraction derives from the weak annihilation diagram induced by the operator O_6 and nonfactorizable contributions [45]. However, the combined effects are not sufficient to reduce f_0 down to 0.5. As can be seen from Table V, our predictions for the longitudinal polarization fractions are generally larger than 0.7, and agree with the previous PQCD calculations from Refs. [52,60]. The small $f_0 \sim (0.50\text{–}0.57)$ in Ref. [62] is ascribed to the inclusion of the higher-power terms proportional to r^2, with r being the mass ratio between the vector and B mesons. The QCDF [38,39] and FAT [64] predictions on the longitudinal polarization fractions are generally less than 0.5. A recent Belle measurement [36] based on the Summer 2020 Belle II

TABLE V. *CP*-averaged branching ratios and polarization fractions for the two-body $B \to \phi K^*$ decays. For comparison, we also list the results from PQCD [52,60,62], QCDF [38,39,61,95], SCET [63], and FAT [64]. The world averages of experimental data are taken from PDG 2020 [37].

Modes	$\mathcal{B}\,(10^{-6})$	f_0 (%)	$f_\perp$ (%)
$B^0 \to \phi K^{*0}$	$7.4^{+2.5+1.1+2.6}_{-2.1-1.2-1.8}$	$74.1^{+3.1+1.5+1.1}_{-5.8-3.0-1.2}$	$13.3^{+3.0+1.6+0.6}_{-1.6-0.8-0.5}$
PQCD-I [52]	14.86	75.0	11.5
PQCD-II [62]	$9.8^{+4.9}_{-3.8}$	$56.5^{+5.8}_{-5.9}$	$21.3^{+2.8}_{-2.9}$
QCDF-I [38]	$9.3^{+0.5+11.4}_{-0.5-6.5}$	44^{+0+59}_{-0-36}	...
QCDF-II [39]	$9.5^{+1.3+11.9}_{-1.2-5.9}$	50^{+50}_{-42}	25^{+21}_{-25}
SCET [63]	9.14 ± 3.14	51.0 ± 16.4	22.2 ± 9.9
FAT [64]	$8.64 \pm 1.76 \pm 1.70 \pm 0.90$	48.0 ± 16.0	26.0 ± 8.6
Data	10.00 ± 0.50	49.7 ± 1.7	22.4 ± 1.5
$B_s^0 \to \phi \bar{K}^{*0}$	$0.12^{+0.04+0.04+0.06}_{-0.03-0.03-0.04}$	$74.5^{+4.6+2.5+3.4}_{-4.8-3.7-6.4}$	$12.7^{+2.4+2.2+3.3}_{-2.5-1.8-1.8}$
PQCD-I [60]	$0.65^{+0.16+1.27+0.10}_{-0.13-0.18-0.04}$	$71.2^{+3.2+2.7+0.0}_{-3.0-3.7-0.0}$	$13.3^{+1.4+1.7+0.0}_{-1.5-1.3-0.0}$
PQCD-II [62]	$0.39^{+0.20}_{-0.17}$	$50.0^{+8.1}_{-7.2}$	$24.2^{+3.6}_{-3.9}$
QCDF-I [38]	$0.4^{+0.1+0.5}_{-0.1-0.3}$	40^{+1+67}_{-1-35}	...
QCDF-II [61]	$0.37^{+0.06+0.24}_{-0.05-0.20}$	43^{+2+21}_{-2-18}	...
QCDF-III [95][a]	$0.11^{+0.07+0.06}_{-0.04-0.01}$	$43.6^{+14.6+51.5}_{-24.0-25.3}$	$25.9^{+8.4+14.4}_{-9.1-23.5}$
SCET [63]	0.56 ± 0.19	54.6 ± 15.0	20.5 ± 9.1
FAT [64]	$0.70 \pm 0.11 \pm 0.13 \pm 0.08$	38.9 ± 14.7	31.4 ± 8.1
Data	1.14 ± 0.30	51.0 ± 17.0	...
$B^+ \to \phi K^{*+}$	$7.6^{+2.9+1.4+2.8}_{-1.8-1.1-1.8}$	$72.3^{+4.4+2.9+2.2}_{-3.9-2.6-0.5}$	$14.3^{+1.9+1.2+0.1}_{-2.2-1.6-1.2}$
PQCD-I [52]	15.96	74.8	11.1
PQCD-II [62]	$10.3^{+4.9}_{-3.8}$	$57.0^{+6.3}_{-5.9}$	$21.0^{+3.0}_{-3.0}$
QCDF-I [38]	$10.1^{+0.5+12.2}_{-0.5-7.1}$	45^{+0+58}_{-0-36}	...
QCDF-II [39]	$10.0^{+1.4+12.3}_{-1.3-6.1}$	49^{+51}_{-42}	25^{+21}_{-25}
SCET [63]	9.86 ± 3.39	51.0 ± 16.4	22.2 ± 9.9
FAT [64]	$9.31 \pm 1.90 \pm 1.83 \pm 0.97$	48.0 ± 16.0	25.9 ± 8.6
Data	10.0 ± 2.0	50.0 ± 5.0	20.0 ± 5.0

[a]We quote the results of case II.

dataset of 34.6 fb^{-1}, yields $f_0(B^0 \to \phi K^{*0}) = 0.57 \pm 0.20 \pm 0.04$ and $f_0(B^+ \to \phi K^{*+}) = 0.58 \pm 0.23 \pm 0.02$, to be compared with our results.

C. *CP*-violating observables

The direct *CP* asymmetry in each component and the overall asymmetry are defined as

$$\mathcal{A}_h^{CP} = \frac{\bar{\mathcal{B}}_h - \mathcal{B}_h}{\bar{\mathcal{B}}_h + \mathcal{B}_h}, \qquad \mathcal{A}_{\rm total}^{CP} = \frac{\sum_h \bar{\mathcal{B}}_h - \sum_h \mathcal{B}_h}{\sum_h \bar{\mathcal{B}}_h + \sum_h \mathcal{B}_h}, \quad (45)$$

respectively. Since only penguin operators work on the neutral channels, there is no direct *CP* asymmetry in the neutral B^0 and B_s^0 modes. However, the charged mode receives an additional tree contribution and the direct *CP* asymmetries arises from the interference between the tree and penguin amplitudes. As shown in Table VI, the direct *CP* asymmetries for various helicity states turn out to be small, $\sim\mathcal{O}(10^{-2})$, and the overall *CP* asymmetry is even lower at the order of 10^{-3}. It can be understood as follows. The tree contribution only appears in the annihilation diagrams, which are power suppressed with respect to the emission ones. Furthermore, the CKM element $|V_{ub}^* V_{us}|$ of

TABLE VI. Direct *CP* asymmetries (in units of %) for the four-body $B^+ \to (K^+K^-)(K^0\pi^+)$ decay. The requirements on the $K\bar{K}$ and $K\pi$ invariant masses are $m_\phi - 0.015 < m_{K\bar{K}} < m_\phi + 0.015$ (GeV) and $m_{K^*} - 0.15 < m_{K\pi} < m_{K^*} + 0.15$ (GeV). The sources of theoretical errors are the same as in previous tables but added in quadrature.

$\mathcal{A}_0^{CP}$	$\mathcal{A}_\parallel^{CP}$	$\mathcal{A}_\perp^{CP}$	$\mathcal{A}_{SS}^{CP}$	$\mathcal{A}_{VS}^{CP}$	$\mathcal{A}_{SV}^{CP}$	$\mathcal{A}_{\rm total}^{CP}$
$-4.1^{+6.1}_{-4.6}$	$5.8^{+2.1}_{-3.8}$	$4.9^{+3.8}_{-4.4}$	$4.5^{+2.0}_{-2.5}$	$3.8^{+2.2}_{-4.2}$	$3.2^{+0.1}_{-4.4}$	$-0.3^{+3.2}_{-2.5}$

TABLE VII. Theoretical predictions of CP violation (in %) for the $B^+ \to \phi K^{*+}$ decay in various approaches.

This work	Data [37]	PQCD [62]	QCDF [38]	QCDF [106]	SCET [63]	FAT [64]
$-1.5^{+4.9}_{-3.3}$	-1 ± 8	-1.0	0^{+0+2}_{-0-1}	0.05	-0.39 ± 0.44	1.00 ± 0.27

tree diagrams is smaller than $|V_{tb}^* V_{ts}|$ of penguin diagrams. Our result in Table VI for the VS and SV components are consistent with the world averages of $(4 \pm 16)\%$ and $(-15 \pm 12)\%$ [37], respectively, within uncertainties.

In Table VII, we list the predicted direct CP asymmetry of the mode $B^+ \to \phi K^{*+}$ in PQCD. For comparison, the experimental data, as well as predictions from previous PQCD [62], QCDF [38,106], SCET [63], and FAT [64], are also presented. All the theoretical approaches show that a nearly vanishing direct CP asymmetry complies with the latest word average of -0.01 ± 0.08 [37] from the measurements [34,107]

$$\mathcal{A}^{CP}(B^+ \to \phi K^{*+}) = \begin{cases} 0.00 \pm 0.09(\text{stat}) \pm 0.04(\text{syst}) & \text{BABAR}, \\ -0.02 \pm 0.14(\text{stat}) \pm 0.03(\text{syst}) & \text{Belle}. \end{cases}$$

Any observation of large direct CP asymmetry to this mode will be a signal for new physics.

TPAs, as mentioned in the Introduction, may be potential signals of CP violation, and thus are complementary to the direct CP violations, particularly when the latter are suppressed by the strong phase. According to Eq. (1), TPAs can be calculated from integrations of the differential decay rate as

$$\begin{aligned}
A_T^1 &= \frac{\Gamma((2\zeta_1-1)(2\zeta_2-1)\sin\varphi>0) - \Gamma((2\zeta_1-1)(2\zeta_2-1)\sin\varphi<0)}{\Gamma((2\zeta_1-1)(2\zeta_2-1)\sin\varphi>0) + \Gamma((2\zeta_1-1)(2\zeta_2-1)\sin\varphi<0)} = -\frac{2\sqrt{2}}{\pi\mathcal{D}} \int d\omega_1 d\omega_2 k(\omega_1) k(\omega_2) k(\omega_1,\omega_2) \text{Im}[A_\perp A_0^*], \\
A_T^2 &= \frac{\Gamma(\sin(2\varphi)>0) - \Gamma(\sin(2\varphi)<0)}{\Gamma(\sin(2\varphi)>0) + \Gamma(\sin(2\varphi)<0)} = -\frac{4}{\pi\mathcal{D}} \int d\omega_1 d\omega_2 k(\omega_1) k(\omega_2) k(\omega_1,\omega_2) \text{Im}[A_\perp A_\parallel^*], \\
A_T^3 &= \frac{\Gamma((2\zeta_1-1)\sin\varphi>0) - \Gamma((2\zeta_1-1)\sin\varphi<0)}{\Gamma((2\zeta_1-1)\sin\varphi>0) + \Gamma((2\zeta_1-1)\sin\varphi<0)} = -\frac{3}{\sqrt{2}\mathcal{D}} \int d\omega_1 d\omega_2 k(\omega_1) k(\omega_2) k(\omega_1,\omega_2) \text{Im}[A_\perp A_{VS}^*], \\
A_T^4 &= \frac{\Gamma((2\zeta_2-1)\sin\varphi>0) - \Gamma((2\zeta_2-1)\sin\varphi<0)}{\Gamma((2\zeta_2-1)\sin\varphi>0) + \Gamma((2\zeta_2-1)\sin\varphi<0)} = -\frac{3}{\sqrt{2}\mathcal{D}} \int d\omega_1 d\omega_2 k(\omega_1) k(\omega_2) k(\omega_1,\omega_2) \text{Im}[A_\perp A_{SV}^*], \\
A_T^5 &= \frac{\Gamma(\sin\varphi>0) - \Gamma(\sin\varphi<0)}{\Gamma(\sin\varphi>0) + \Gamma(\sin\varphi<0)} = -\frac{9\pi}{4\sqrt{2}\mathcal{D}} \int d\omega_1 d\omega_2 k(\omega_1) k(\omega_2) k(\omega_1,\omega_2) \text{Im}[A_\perp A_{SS}^*],
\end{aligned} \tag{46}$$

with

$$\mathcal{D} = \int d\omega_1 d\omega_2 k(\omega_1) k(\omega_2) k(\omega_1,\omega_2) \sum_h Y_h |A_h|^2, \tag{47}$$

where the mass integration extends over the chosen mass window. It is seen that the TPAs are produced by the interference between $A_\perp$ and A_i with $i = 0, \parallel, SV, VS, SS$ and take the form $\text{Im}(A_\perp A_i^*) = |A_\perp||A_i^*| \sin(\Delta\phi + \Delta\delta)$, where $\Delta\phi$ and $\Delta\delta$, respectively, denote weak and strong phase differences between the two amplitudes. Here the strong phase difference could produce a nonzero value, even if the weak phases vanish. Thus, a nonzero TPA is not necessarily a signal of CP violation. In order to obtain a true signal of CP violation, one has to compare the TPAs in B and $\bar{B}$ decays. The helicity amplitudes for the CP-conjugated process can be obtained by applying the following transformations:

$$\begin{aligned}
&A_0 \to \bar{A}_0, A_\parallel \to \bar{A}_\parallel, A_\perp \to -\bar{A}_\perp, A_{SV} \to \bar{A}_{SV}, \\
&A_{VS} \to \bar{A}_{VS}, A_{SS} \to \bar{A}_{SS}.
\end{aligned} \tag{48}$$

Then, the associated TPAs for the charge-conjugate process, $\bar{A}_T^i$, are defined similarly. Now, we can construct the true and fake asymmetries by combining A_T^i and $\bar{A}_T^i$ [3]

$$\begin{aligned}
A_T^i(\text{true}) &= \frac{1}{2}(A_T^i + \bar{A}_T^i) \propto \sin(\Delta\phi)\cos(\Delta\delta), \\
A_T^i(\text{fake}) &= \frac{1}{2}(A_T^i - \bar{A}_T^i) \propto \cos(\Delta\phi)\sin(\Delta\delta).
\end{aligned} \tag{49}$$

It was pointed out in Ref. [9] that the second equation above is valid only in the absence of direct CP asymmetry

in the total decay rate. As the total direct *CP* asymmetry does not exceed a few percent as shown in Table VI, the above approximation holds in $B \to \phi K^*$ decays. It is clear that $A_T^i(\text{true})$ do not suffer the suppression from the strong phase $\Delta\delta$ compared with the direct *CP* violation. It is nonzero only if the weak phases are nonzero, and provides a measure for *CP* violation. Nevertheless, $A_T^i(\text{fake})$ can be nonzero even if the weak phases are zero. Such a quantity will sometimes be referred to as a fake asymmetry. It reflects the importance of strong final-state phases [9], and thus is not a signal of *CP* violation. Since the helicity amplitudes always have different strong phases, this will lead to nonzero fake TPAs for all decays.

The calculated TPAs for the concerned decays are collected in Table VIII. In the special case of the involved neutral intermediate states $B^0 \to \phi K^{*0}$ and $B_s^0 \to \phi \bar{K}^{*0}$ modes, in which each helicity amplitude involves the same single weak phase in the SM. This results in $A_T^i = -\bar{A}_T^i$ due to the vanishing weak phase difference. The true TPAs for the two neutral modes are thus expected to be zero as shown in Table VIII. If such asymmetries are observed experimentally, it is probably a signal of new physics. The situation of the fake TPAs is different. Many nonzero and even sizable fake TPAs are predicted in our calculations. The magnitude of $A_T^1(\text{fake})$ for the B^0 and B^+ channels exceeds ten percent, even reaching 24.0% for the B_s one, whereas the *S*-wave induced fake TPAs, $A_T^{3,4,5}(\text{fake})$, are predicted to be several percent. The smallness of $A_T^2(\text{fake})$ is caused by the suppression from the strong phase difference between the perpendicular and parallel polarization amplitudes, which are found to be very close to 0 in PQCD framework [60,62]. Hence, the measurement of a large A_T^2 would point clearly towards the presence of new physics beyond the SM.

Experimentally, an complete angular analysis of the decay $B^0 \to \phi K^{*0}$ is available from LHCb [58], *BABAR* [31,32], and Belle [34,35] Collaborations, which allows us to determine the true and fake TPAs from the measured polarization amplitudes, phases, and amplitude differences between B^0 and $\bar{B}^0$ decays. The concerned decays are all self-tagged processes, whose triple product asymmetry can be computed separately for B and $\bar{B}$ decays. We note that the definitions of the *CP* asymmetries and TPAs are different among these measurements. To compare these results directly, it is necessary to rescale them with the unified definitions. We follow the convention of Ref. [9], defining

$$(A_T^1)_{\text{exp}} = -\frac{2\sqrt{2}}{\pi}\frac{\text{Im}(A_\perp A_0^*)}{|A_0|^2+|A_\parallel|^2+|A_\perp|^2},$$
$$(A_T^2)_{\text{exp}} = -\frac{4}{\pi}\frac{\text{Im}(A_\perp A_\parallel^*)}{|A_0|^2+|A_\parallel|^2+|A_\perp|^2}. \quad (50)$$

TABLE VIII. PQCD predictions for the TPAs(%). The mass of the $K\bar{K}(K\pi)$ pair is required to be within 15 MeV (150 MeV) of the known $\phi(K^*)$ meson mass.

Asymmetries	$B^0 \to (K^+K^-)(K^+\pi^-)$	$B_s^0 \to (K^+K^-)(K^-\pi^+)$	$B^+ \to (K^+K^-)(K^0\pi^+)$
A_T^1	$-13.8^{+4.8}_{-4.3}$	$-24.0^{+6.6}_{-3.8}$	$-14.1^{+5.0}_{-3.8}$
$\bar{A}_T^1$	$13.8^{+4.8}_{-4.3}$	$24.0^{+6.6}_{-3.8}$	$+13.8^{+5.6}_{-3.9}$
$A_T^1(\text{true})$	0.0	0.0	$-0.15^{+0.05}_{-0.30}$
$A_T^1(\text{fake})$	$-13.8^{+4.8}_{-4.3}$	$-24.0^{+6.6}_{-3.8}$	$-14.0^{+5.3}_{-3.9}$
A_T^2	$-0.3^{+0.1}_{-0.1}$	$-0.1^{+0.0}_{-0.0}$	$-0.3^{+0.1}_{-0.1}$
$\bar{A}_T^2$	$0.3^{+0.1}_{-0.1}$	$0.1^{+0.0}_{-0.0}$	$0.2^{+0.1}_{-0.0}$
$A_T^2(\text{true})$	0.0	0.0	$-0.05^{+0.00}_{-0.05}$
$A_T^2(\text{fake})$	$-0.3^{+0.1}_{-0.1}$	$-0.1^{+0.0}_{-0.0}$	$-0.3^{+0.1}_{-0.1}$
A_T^3	$-5.4^{+1.0}_{-0.6}$	$-6.4^{+2.1}_{-2.2}$	$-5.6^{+1.0}_{-0.6}$
$\bar{A}_T^3$	$5.4^{+1.0}_{-0.6}$	$6.4^{+2.1}_{-2.2}$	$5.5^{+1.0}_{-0.6}$
$A_T^3(\text{true})$	0.0	0.0	$-0.05^{+0.00}_{-0.00}$
$A_T^3(\text{fake})$	$-5.4^{+1.0}_{-0.6}$	$-6.4^{+2.1}_{-2.2}$	$-5.6^{+1.0}_{-0.6}$
A_T^4	$1.6^{+3.0}_{-3.0}$	$-8.1^{+3.2}_{-3.3}$	$1.6^{+3.2}_{-2.7}$
$\bar{A}_T^4$	$-1.6^{+3.0}_{-3.0}$	$8.1^{+3.2}_{-3.3}$	$-1.8^{+3.1}_{-2.8}$
$A_T^4(\text{true})$	0.0	0.0	$-0.10^{+0.05}_{-0.00}$
$A_T^4(\text{fake})$	$1.6^{+3.0}_{-3.0}$	$-8.1^{+3.2}_{-3.3}$	$1.7^{+3.2}_{-2.8}$
A_T^5	$-4.3^{+1.1}_{-0.8}$	$-6.7^{+1.8}_{-1.9}$	$-4.2^{+1.1}_{-0.8}$
$\bar{A}_T^5$	$4.3^{+1.1}_{-0.8}$	$6.7^{+1.8}_{-1.9}$	$4.3^{+1.2}_{-0.8}$
$A_T^5(\text{true})$	0.0	0.0	$0.05^{+0.00}_{-0.05}$
$A_T^5(\text{fake})$	$-4.3^{+1.1}_{-0.8}$	$-6.7^{+1.8}_{-1.9}$	$-4.3^{+1.2}_{-0.8}$

TABLE IX. Comparison of measurements in the angular analysis of $B^0 \to \phi K^{*0}$ made by *BABAR* [32], Belle [35], and LHCb [58] experiments, where the first and second uncertainties are statistical and systematic, respectively. The true and fake TPAs for the P-wave components are deduced from the fitted parameters (the first eight lines), while the S-wave ones are taken from LHCb [58].

Parameters	*BABAR*	Belle	LHCb
f_L	$0.494 \pm 0.034 \pm 0.013$	$0.499 \pm 0.030 \pm 0.018$	$0.497 \pm 0.019 \pm 0.015$
$f_\perp$	$0.212 \pm 0.032 \pm 0.013$	$0.238 \pm 0.026 \pm 0.008$	$0.221 \pm 0.016 \pm 0.013$
$\delta_\perp$	$2.35 \pm 0.13 \pm 0.09$	$2.37 \pm 0.10 \pm 0.04$	$2.633 \pm 0.062 \pm 0.037$
$\delta_\parallel$	$2.40 \pm 0.13 \pm 0.08$	$2.23 \pm 0.10 \pm 0.02$	$2.562 \pm 0.069 \pm 0.040$
A_0^{CP}	$+0.01 \pm 0.07 \pm 0.02$	$-0.030 \pm 0.061 \pm 0.007$	$-0.003 \pm 0.038 \pm 0.005$
$A_\perp^{CP}$	$-0.04 \pm 0.15 \pm 0.06$	$-0.14 \pm 0.11 \pm 0.01$	$+0.047 \pm 0.072 \pm 0.009$
$\delta_\perp^{CP}$	$+0.21 \pm 0.13 \pm 0.08$	$+0.05 \pm 0.10 \pm 0.02$	$+0.062 \pm 0.062 \pm 0.006$
$\delta_\parallel^{CP}$	$+0.22 \pm 0.12 \pm 0.08$	$-0.02 \pm 0.10 \pm 0.01$	$+0.045 \pm 0.068 \pm 0.015$
Asymmetries	*BABAR*	Belle	LHCb
A_T^1(true)	$-0.046 \pm 0.031 \pm 0.017$	$-0.029 \pm 0.025 \pm 0.005$	$-0.007 \pm 0.012 \pm 0.002$
A_T^2(true)	$-0.003 \pm 0.056 \pm 0.036$	$0.021 \pm 0.040 \pm 0.006$	$+0.004 \pm 0.014 \pm 0.002$
A_T^3(true)	⋯	⋯	$+0.004 \pm 0.006 \pm 0.001$
A_T^4(true)	⋯	⋯	$+0.002 \pm 0.006 \pm 0.001$
A_T^1(fake)	$-0.203 \pm 0.031 \pm 0.019$	$-0.211 \pm 0.025 \pm 0.010$	$-0.105 \pm 0.012 \pm 0.006$
A_T^2(fake)	$0.016 \pm 0.058 \pm 0.038$	$-0.041 \pm 0.040 \pm 0.013$	$-0.017 \pm 0.014 \pm 0.003$
A_T^3(fake)	⋯	⋯	$-0.063 \pm 0.006 \pm 0.005$
A_T^4(fake)	⋯	⋯	$-0.019 \pm 0.006 \pm 0.007$

The corresponding quantities for the charge-conjugate process, $(\bar{A}_T^{1,2})_{\rm exp}$, are defined similarly. We can calculate the true and fake asymmetries from Eq. (49). The measured polarizations, phases, and CP violation asymmetries as well as the true and fake TPAs of $B^0 \to \phi K^{*0}$ by the LHCb, *BABAR*, and Belle Collaborations are compared in Table IX. One can see that all the true asymmetries are measured to be consistent with zero, showing no evidence for CP violation. Nevertheless, a significant fake asymmetry, such as A_T^1(fake), is observed in all three different experiments, reflecting the importance of final-state interactions. The S-wave induced TPAs, which arise from the interference between $A_\perp$ and one S-wave amplitude, have not been determined in *BABAR* and Belle, since the contributions of S-wave $K\bar{K}$ and $K\pi$ and their interferences were not fully included into the angular analysis. It is pointed out that contributions from the S-wave $K\bar{K}$ and $K\pi$ are significant and should be taken into account in future measurements. The three additional CP-violating observables can then provide valuable complementary information on NP.

The only available amplitude analysis of $B^+ \to \phi K^{*+}$ was performed by the *BABAR* [107] experiment. The fitted polarization parameters together with the true and fake TPAs are summarized in Table X. The S-wave $K\pi$ contribution was included to resolve the twofold phase ambiguity, but the accurate assessments of the S-wave component have not been determined, leading to the corresponding S-wave induced TPAs still being absent.

Although the polarization fractions and branching ratio of the decay $B_s^0 \to \phi \bar{K}^{*0}$ have been measured by the LHCb experiment [59], the full angular analysis has not been done because of the limited signal events, which results in the measurement on TPAs not being available yet. As indicated in Table VIII, the predicted large fake TPAs for the B_s mode would be tested in the future.

TABLE X. Parameters measured in the angular analysis of $B^+ \to \phi K^{*+}$ by *BABAR* [107], where the first and second uncertainties are statistical and systematic, respectively. The true and fake TPAs (the last four entries) are deduced from the fitted parameters (the first eight lines).

Parameters	*BABAR*
f_L	$+0.49 \pm 0.05 \pm 0.03$
$f_\perp$	$+0.21 \pm 0.05 \pm 0.02$
$\delta_\perp - \pi$	$-0.45 \pm 0.20 \pm 0.03$
$\delta_\parallel - \pi$	$-0.67 \pm 0.20 \pm 0.07$
A_0^{CP}	$+0.17 \pm 0.11 \pm 0.02$
$A_\perp^{CP}$	$+0.22 \pm 0.24 \pm 0.08$
$\delta_\perp^{CP}$	$+0.19 \pm 0.20 \pm 0.07$
$\delta_\parallel^{CP}$	$+0.07 \pm 0.20 \pm 0.05$
Asymmetries	*BABAR*
A_T^1(true)	$-0.025 \pm 0.056 \pm 0.019$
A_T^2(true)	$0.028 \pm 0.084 \pm 0.026$
A_T^1(fake)	$-0.114 \pm 0.056 \pm 0.011$
A_T^2(fake)	$-0.061 \pm 0.084 \pm 0.023$

IV. CONCLUSION

B meson four-body decays provide a wealth of information on the weak interactions, in terms of a number of observables ranging from the branching ratios, polarizations, CP asymmetries, and triple product asymmetries to a full angular analysis. In this work, we have concentrated on the penguin-dominated $B_{(s)} \to \phi(\to K\bar{K})K^*(\to K\pi)$ decays using the perturbative QCD approach. The calculations were performed in the $K\bar{K}(K\pi)$ invariant mass window of 15(150) MeV around the $\phi(K^*)$ mass. In addition to the dominant vector resonances, four-particle final states can also be obtained through one or two scalar meson intermediate states in the given mass regions. The strong dynamics of the scalar or vector resonance decays into the meson pair was parametrized into the corresponding two-meson DAs, which has been well established in three-body B meson decays. Angular momentum conservation in the decay allows for three amplitudes for vector-vector decays and one single amplitude in modes involving at least one scalar $K\bar{K}(K\pi)$ pair. The CP-averaged branching ratios of all components were predicted in the chosen mass ranges. The single S-wave contributions were found to be significant and consistent with the data from the LHCb experiment, while the double S-wave contributions were only a few percent in the considered invariant mass range. It has been demonstrated that the S-wave contributions were strongly sensitive to the integrating ranges. After choosing the same $K\pi$ mass range, our results can be comparable with the Belle and *BABAR* measurements roughly.

We extracted the two-body $B \to \phi K^*$ branching ratios from the results for the corresponding quasi-two-body modes by employing the narrow width approximation. The obtained results basically agree with previous predictions performed in the two-body framework within theoretical uncertainty. However, various predictions for $\mathcal{B}(B_s^0 \to \phi\bar{K}^{*0})$ lie in a wide range, generally below the current world average value. The gap between theory and experiment requires a more thorough study. The longitudinal polarization fractions were estimated to be $f_0 \sim 0.7$, somewhat lower than the naive expectation of a dominant longitudinal polarization because of the important chirally enhanced annihilation and nonfactorizable contributions. However, the observation of an even smaller value of 0.5 by Belle, *BABAR*, and LHCb, means the existing explanations of the abnormal polarization are not satisfactory and thus call for more in-depth studies.

We have also investigated the direct CP asymmetries and TPAs in the $B \to (K\bar{K})(K\pi)$ decays. For the two pure-penguin neutral channels, both the direct CP asymmetries and true TPAs should be zero in SM due to the vanishing weak phase difference. It was observed that the direct CP asymmetries for the charged modes are small, of order 10^{-2}, since the tree contributions are significantly suppressed compared to the penguin ones. A similar observation was made in previous PQCD, QCDF, SCET, and FAT approaches and supported by the measurements from *BABAR* and Belle. The true TPAs are predicted to be tiny, of order 10^{-3}, compatible with the absence of CP violation, whereas, the fake TPAs were found to be sizable, which can provide valuable information on final-state interactions.

The full angular analysis of $B^0 \to \phi K^{*0}$ has been performed by LHCb, *BABAR*, and Belle experiments, and allow one to derive the true and fake TPAs from the results of the angular analysis. It is worth noting that the S-wave components and their interference have not been fully considered into the analysis in *BABAR* and Belle experiments. Therefore, the only available measurements for the S-wave induced TPAs are from LHCb. By including the S-wave $K\bar{K}$ and $K\pi$ components, we have estimated the S-wave induced TPAs for the first time. The predicted asymmetries $B^0 \to \phi K^{*0}$ are in good agreement with those reported by the LHCb. As the three additional CP-violating observables may provide valuable complementary information on NP, a dedicated angular analysis from Belle and *BABAR* data is expected. The full angular analysis of $B_s^0 \to \phi\bar{K}^{*0}$ was still not available due to the limited samples. The obtained asymmetries can be confronted with the future data.

The experimental measurement may be improved by expanding the mass region to around 1.5 GeV based on more precise data in the future. Then the angular analysis could include the contributions of some higher excited intermediate states, such as D-wave $K_2^*(1430)$, P-wave $\phi(1680)$, and S-wave $f_0(1370)$, and so on. The additional contributions and their interferences would provide a lot of meaningful asymmetries in angular distributions, and leading to the amplitude analysis will be more complicated and complete. This is an intriguing topic for future investigation.

ACKNOWLEDGMENTS

This work is supported by National Natural Science Foundation of China under Grants No. 12075086, No. 12005103, and No. 11605060. Z. R. is supported in part by the Natural Science Foundation of Hebei Province under Grants No. A2021209002 and No. A2019209449. Y. L. is also supported by the Natural Science Foundation of Jiangsu Province under Grant No. BK20190508 and the Research Start-up Funds of Nanjing Agricultural University.

APPENDIX: DECAY AMPLITUDES

Here we present the helicity amplitudes for the concerned channels as follows:

$$\begin{aligned}\mathcal{A}_h(B^0\to\phi(\to K^+K^-)K^{*0}(\to K^+\pi^-)) =& \frac{G_F}{\sqrt{2}}V_{tb}^*V_{ts}X_h\left\{\frac{4}{3}\left[C_3+C_4-\frac{1}{2}(C_9+C_{10})\right]\mathcal{F}_e^{LL}+\left[C_5+\frac{1}{3}C_6-\frac{1}{2}\left(C_7+\frac{1}{3}C_8\right)\right]\mathcal{F}_e^{LR}\right.\\ &+\left[C_6+\frac{1}{3}C_5-\frac{1}{2}\left(C_8+\frac{1}{3}C_7\right)\right]\mathcal{F}_e^{SP}+\left[C_3+C_4-\frac{1}{2}(C_9+C_{10})\right]\mathcal{M}_e^{LL}\\ &+\left(C_5-\frac{1}{2}C_7\right)\mathcal{M}_e^{LR}+\left(C_6-\frac{1}{2}C_8\right)\mathcal{M}_e^{SP}+\left[C_4+\frac{1}{3}C_3-\frac{1}{2}\left(C_{10}+\frac{1}{3}C_9\right)\right]\mathcal{F}_a^{LL}\\ &\left.+\left[C_6+\frac{1}{3}C_5-\frac{1}{2}\left(C_8+\frac{1}{3}C_7\right)\right]\mathcal{F}_a^{SP}+\left(C_3-\frac{1}{2}C_9\right)\mathcal{M}_a^{LL}+\left(C_5-\frac{1}{2}C_7\right)\mathcal{M}_a^{LR}\right\},\end{aligned} \tag{A1}$$

$$\begin{aligned}\mathcal{A}_h(B_s^0\to\phi(\to K^+K^-)\bar{K}^{*0}(\to K^-\pi^+)) =& \frac{G_F}{\sqrt{2}}V_{tb}^*V_{td}X_h\left\{\left[C_3+\frac{1}{3}C_4-\frac{1}{2}\left(C_9+\frac{1}{3}C_{10}\right)\right]\mathcal{F}_e^{LL}\right.\\ &+\left[C_4+\frac{1}{3}C_3-\frac{1}{2}\left(C_{10}+\frac{1}{3}C_9\right)\right]\mathcal{F}_e'^{LL}+\left[C_6+\frac{1}{3}C_5-\frac{1}{2}\left(C_8+\frac{1}{3}C_7\right)\right]\mathcal{F}_e'^{SP}\\ &+\left[C_5+\frac{1}{3}C_6-\frac{1}{2}\left(C_7+\frac{1}{3}C_8\right)\right]\mathcal{F}_e^{LR}+\left(C_4-\frac{1}{2}C_{10}\right)\mathcal{M}_e^{LL}+\left(C_3-\frac{1}{2}C_9\right)\mathcal{M}_e'^{LL}\\ &+\left(C_6-\frac{1}{2}C_8\right)\mathcal{M}_e^{SP}+\left(C_5-\frac{1}{2}C_7\right)\mathcal{M}_e'^{LR}+\left[C_4+\frac{1}{3}C_3-\frac{1}{2}\left(C_{10}+\frac{1}{3}C_9\right)\right]\mathcal{F}_a'^{LL}\\ &\left.+\left[C_6+\frac{1}{3}C_5-\frac{1}{2}\left(C_8+\frac{1}{3}C_7\right)\right]\mathcal{F}_a'^{SP}+\left(C_3-\frac{1}{2}C_9\right)\mathcal{M}'^{LL}_a+\left(C_5-\frac{1}{2}C_7\right)\mathcal{M}_a'^{LR}\right\},\end{aligned} \tag{A2}$$

$$\begin{aligned}\mathcal{A}_h(B^+\to\phi(\to K^+K^-)K^{*+}(\to K^0\pi^+)) =& \frac{G_F}{\sqrt{2}}V_{ub}^*V_{us}X_h\left\{\left(C_2+\frac{1}{3}C_1\right)\mathcal{F}_a^{LL}+(C_1)\mathcal{M}_a^{LL}\right\}\\ &-\frac{G_F}{\sqrt{2}}V_{tb}^*V_{ts}X_h\left\{\frac{4}{3}\left[C_3+C_4-\frac{1}{2}(C_9+C_{10})\right]\mathcal{F}_e^{LL}+\left[C_5+\frac{1}{3}C_6-\frac{1}{2}\left(C_7+\frac{1}{3}C_8\right)\right]\mathcal{F}_e^{LR}\right.\\ &+\left[C_6+\frac{1}{3}C_5-\frac{1}{2}\left(C_8+\frac{1}{3}C_7\right)\right]\mathcal{F}_e^{SP}+\left[C_3+C_4-\frac{1}{2}(C_9+C_{10})\right]\mathcal{M}_e^{LL}\\ &+\left(C_5-\frac{1}{2}C_7\right)\mathcal{M}_e^{LR}+\left(C_6-\frac{1}{2}C_8\right)\mathcal{M}_e^{SP}+\left[C_4+\frac{1}{3}C_3+C_{10}+\frac{1}{3}C_9\right]\mathcal{F}_a^{LL}\\ &\left.+\left[C_6+\frac{1}{3}C_5+C_8+\frac{1}{3}C_7\right]\mathcal{F}_a^{SP}+(C_3+C_9)\mathcal{M}_a^{LL}+(C_5+C_7)\mathcal{M}_a^{LR}\right\},\end{aligned} \tag{A3}$$

with

$$X_h=\begin{cases}\sqrt{1+4\alpha_1}\sqrt{1+4\alpha_2}, & h=0,\parallel,\perp\\ \sqrt{1+4\alpha_{1,2}}, & h=SV,VS\\ 1, & h=SS.\end{cases} \tag{A4}$$

The explicit expressions of $\mathcal{F}/\mathcal{M}$ can be found in [15]. Note that the term $\mathcal{F}_e^{SP}$ from the operators O_{5-8} vanishes when a vector resonance is emitted from the weak vertex, because neither the scalar nor the pseudoscalar density gives contributions to the vector resonance production.

[1] N. Sinha and R. Sinha, Determination of the *CP* violation angle γ using $B \to D^* V$ modes, Phys. Rev. Lett. **80**, 3706 (1998).

[2] G. Kramer and W. F. Palmer, Branching ratios and *CP* asymmetries in the decay $B \to VV$, Phys. Rev. D **45**, 193 (1992).

[3] E. Kou *et al.* (Belle II Collaboration), The Belle-II physics book, Prog. Theor. Exp. Phys. **2019**, 123C01 (2019); Erratum, **2020**, 029201 (2020).

[4] S. Stone and L. Zhang, *S* waves and the measurement of *CP* violating phases in B_s decays, Phys. Rev. D **79**, 074024 (2009).

[5] Y. Xie, P. Clarke, G. Cowan, and F. Muheim, Determination of $2\beta_s$ in $B_s^0 \to J/\psi K^+ K^-$ decays in the presence of a K^+K^- *S*-wave contribution, J. High Energy Phys. 09 (2009) 074.

[6] B. Bhattacharya, A. Datta, M. Duraisamy, and D. London, Searching for new physics with $\bar{b} \to \bar{s}$ $B_s^0 \to V_1 V_2$ penguin decays, Phys. Rev. D **88**, 016007 (2013).

[7] W. Bensalem and D. London, *T*-violating triple-product correlations in hadronic *b* decays, Phys. Rev. D **64**, 116003 (2001).

[8] A. Datta and D. London, Triple-product correlations in $B \to V_1 V_2$ decays and new physics, Int. J. Mod. Phys. A **19**, 2505 (2004).

[9] M. Gronau and J. L. Rosner, Triple product asymmetries in K, $D_{(s)}$ and $B_{(s)}$ decays, Phys. Rev. D **84**, 096013 (2011).

[10] A. Datta, M. Duraisamy, and D. London, Searching for new physics with B-decay fake triple products, Phys. Lett. B **701**, 357 (2011).

[11] A. Datta, M. Duraisamy, and D. London, New physics in $\bar{b} \to \bar{s}$ transitions and the $B_{d,s}^0 \to V_1 V_2$ angular analysis, Phys. Rev. D **86**, 076011 (2012).

[12] S. K. Patra and A. Kundu, *CPT* violation and triple-product correlations in B decays, Phys. Rev. D **87**, 116005 (2013).

[13] G. Durieux and Y. Grossman, Probing *CP* violation systematically in differential distributions, Phys. Rev. D **92**, 076013 (2015).

[14] A. J. Bevan, C, P, and CP asymmetry observables based on triple product asymmetries, arXiv:1408.3813.

[15] Z. Rui, Y. Li, and H. n. Li, Four-body decays $B_{(s)} \to (K\pi)_{S/P}(K\pi)_{S/P}$ in the perturbative QCD approach, J. High Energy Phys. 05 (2021) 082.

[16] Y. Li, D. C. Yan, Z. Rui, and Z. J. Xiao, Study of $B_{(s)} \to (\pi\pi)(K\pi)$ decays in the perturbative QCD approach, Eur. Phys. J. C **81**, 806 (2021).

[17] W. F. Wang, H. n. Li, W. Wang, and C. D. Lü, *S*-wave resonance contributions to the $B_{(s)}^0 \to J/\psi \pi^+ \pi^-$ and $B_s \to \pi^+\pi^-\mu^+\mu^-$ decays, Phys. Rev. D **91**, 094024 (2015).

[18] S. Kränkl, T. Mannel, and J. Virto, Three-body nonleptonic B decays and QCD factorization, Nucl. Phys. **B899**, 247 (2015).

[19] D. Boito, J. P. Dedonder, B. El-Bennich, R. Escribano, R. Kaminski, L. Lesniak, and B. Loiseau, Parametrizations of three-body hadronic *B*- and *D*-decay amplitudes in terms of analytic and unitary meson-meson form factors, Phys. Rev. D **96**, 113003 (2017).

[20] A. G. Grozin, On wave functions of meson pairs and meson resonances, Sov. J. Nucl. Phys. **38**, 289 (1983).

[21] A. G. Grozin, One- and two-particle wave functions of multihadron systems, Theor. Math. Phys. **69**, 1109 (1986).

[22] D. Müller, D. Robaschik, B. Geyer, F.-M. Dittes, and J. Hořejši, Wave functions, evolution equations and evolution kernels from light ray operators of QCD, Fortschr. Phys. **42**, 101 (1994).

[23] M. Diehl, T. Gousset, B. Pire, and O. Teryaev, Probing Partonic Structure in $\gamma^*\gamma \to \pi\pi$ Near Threshold, Phys. Rev. Lett. **81**, 1782 (1998).

[24] M. Diehl, T. Gousset, and B. Pire, Exclusive production of pion pairs in $\gamma^*\gamma$ collisions at large Q^2, Phys. Rev. D **62**, 073014 (2000).

[25] B. Pire and L. Szymanowski, Impact representation of generalized distribution amplitudes, Phys. Lett. B **556**, 129 (2003).

[26] M. V. Polyakov, Hard exclusive electroproduction of two pions and their resonances, Nucl. Phys. **B555**, 231 (1999).

[27] C. H. Chen and H. n. Li, Three body nonleptonic B decays in perturbative QCD, Phys. Lett. B **561**, 258 (2003).

[28] R. A. Briere *et al.* (CLEO Collaboration), Observation of $B \to \phi K$ and $B \to \phi K^*$, Phys. Rev. Lett. **86**, 3718 (2001).

[29] B. Aubert *et al.* (*BABAR* Collaboration), Rates, Polarizations, and Asymmetries in Charmless Vector-Vector *B* Meson Decays, Phys. Rev. Lett. **91**, 171802 (2003).

[30] B. Aubert *et al.* (*BABAR* Collaboration), Measurement of the $B^0 \to \phi K^0$ Decay Amplitudes, Phys. Rev. Lett. **93**, 231804 (2004).

[31] B. Aubert *et al.* (*BABAR* Collaboration), Vector-Tensor and Vector-Vector Decay Amplitude Analysis of $B^0 \to \phi K^{*0}$, Phys. Rev. Lett. **98**, 051801 (2007).

[32] B. Aubert *et al.* (*BABAR* Collaboration), Time-dependent and time-integrated angular analysis of $B \to \phi K_S^0 \pi^0$ and $B \to \phi K^{\pm}\pi^{\mp}$, Phys. Rev. D **78**, 092008 (2008).

[33] K. F. Chen *et al.* (Belle Collaboration), Measurement of Branching Fractions and Polarization in $B \to \phi K^{(*)}$ Decays, Phys. Rev. Lett. **91**, 201801 (2003).

[34] K. F. Chen *et al.* (Belle Collaboration), Measurement of Polarization and Triple-Product Correlations in $B \to \phi K^*$ Decays, Phys. Rev. Lett. **94**, 221804 (2005).

[35] M. Prim *et al.* (Belle Collaboration), Angular analysis of $B^0 \to \phi K^*$ decays and search for *CP* violation at Belle, Phys. Rev. D **88**, 072004 (2013).

[36] F. Abudinén *et al.* (Belle-II Collaboration), Rediscovery of $B \to \phi K^{(*)}$ decays and measurement of the longitudinal polarization fraction f_L in $B \to \phi K^*$ decays using the Summer 2020 Belle II dataset, arXiv:2008.03873.

[37] Particle Data Group, Review of particle physics, Prog. Theor. Exp. Phys. **2020**, 083C01 (2020).

[38] M. Beneke, J. Rohrer, and D. Yang, Branching fractions, polarisation and asymmetries of $B \to VV$ decays, Nucl. Phys. **B774**, 64 (2007).

[39] H. Y. Cheng and K. C. Yang, Branching ratios and polarization in $B \to VV, VA, AA$ decays, Phys. Rev. D **78**, 094001 (2008); Erratum, **79**, 039903 (2009).

[40] Y. Grossman, Beyond the standard model with B and K physics, Int. J. Mod. Phys. A **19**, 907 (2004).

[41] P. K. Das and K. C. Yang, Data for polarization in charmless $B \to \phi K^*$: A signal for new physics?, Phys. Rev. D **71**, 094002 (2005).

[42] C. H. Chen and C. Q. Geng, Scalar interactions to the polarizations of $B \to \phi K^*$, Phys. Rev. D **71**, 115004 (2005).

[43] Y. D. Yang, R. M. Wang, and G. R. Lu, Polarizations in decays $B_{u,d} \to VV$ and possible implications for R-parity violating SUSY, Phys. Rev. D **72**, 015009 (2005).

[44] A. L. Kagan, Polarization in $B \to VV$ decays, Phys. Lett. B **601**, 151 (2004).

[45] H. n. Li and S. Mishima, Polarizations in $B \to VV$ decays, Phys. Rev. D **71**, 054025 (2005).

[46] M. Beneke, J. Rohrer, and D. Yang, Enhanced Electroweak Penguin Amplitude in $B \to VV$ Decays, Phys. Rev. Lett. **96**, 141801 (2006).

[47] A. Datta, A. V. Gritsan, D. London, M. Nagashima, and A. Szynkman, Testing explanations of the $B \to \phi K^*$ polarization puzzle, Phys. Rev. D **76**, 034015 (2007).

[48] C. W. Bauer, D. Pirjol, I. Z. Rothstein, and I. W. Stewart, $B \to M_1 M_2$: Factorization, charming penguins, strong phases, and polarization, Phys. Rev. D **70**, 054015 (2004).

[49] P. Colangelo, F. De Fazio, and T. N. Pham, The riddle of polarization in $B \to VV$ transitions, Phys. Lett. B **597**, 291 (2004).

[50] M. Ladisa, V. Laporta, G. Nardulli, and P. Santorelli, Final state interactions for $B \to VV$ charmless decays, Phys. Rev. D **70**, 114025 (2004).

[51] H. Y. Cheng, C. K. Chua, and A. Soni, Final state interactions in hadronic B decays, Phys. Rev. D **71**, 014030 (2005).

[52] C. H. Chen, Y. Y. Keum, and H. n. Li, Perturbative QCD analysis of $B \to \phi K^*$ decays, Phys. Rev. D **66**, 054013 (2002).

[53] H. n. Li, Resolution to the $B \to \phi K^*$ polarization puzzle, Phys. Lett. B **622**, 63 (2005).

[54] W. S. Hou and M. Nagashima, Resolving the $B \to \phi K^*$ polarization anomaly, arXiv:hep-ph/0408007.

[55] W. j. Zou and Z. j. Xiao, Charmless $B \to PV, VV$ decays and new physics effects in the mSUGRA model, Phys. Rev. D **72**, 094026 (2005).

[56] Q. Chang, X. Q. Li, and Y. D. Yang, Constraints on the anomalous tensor operators from $B \to \phi K^*, \eta K^*$, and ηK decays, J. High Energy Phys. 06 (2007) 038.

[57] S. S. Bao, F. Su, Y. L. Wu, and C. Zhuang, Exclusive $B \to VV$ decays and CP violation in the general two-Higgs-doublet model, Phys. Rev. D **77**, 095004 (2008).

[58] R. Aaij *et al.* (LHCb Collaboration), Measurement of polarization amplitudes and CP asymmetries in $B^0 \to \phi K^*(892)^0$, J. High Energy Phys. 05 (2014) 069.

[59] R. Aaij *et al.* (LHCb Collaboration), First observation of the decay $B_s^0 \to \phi \bar{K}^{*0}$, J. High Energy Phys. 11 (2013) 092.

[60] A. Ali, G. Kramer, Y. Li, C. D. Lu, Y. L. Shen, W. Wang, and Y. M. Wang, Charmless non-leptonic B_s decays to PP, PV and VV final states in the pQCD approach, Phys. Rev. D **76**, 074018 (2007).

[61] H. Y. Cheng and C. K. Chua, QCD factorization for charmless hadronic B_s decays revisited, Phys. Rev. D **80**, 114026 (2009).

[62] Z. T. Zou, A. Ali, C. D. Lu, X. Liu, and Y. Li, Improved estimates of the $B_{(s)} \to VV$ decays in perturbative QCD approach, Phys. Rev. D **91**, 054033 (2015).

[63] C. Wang, S. H. Zhou, Y. Li, and C. D. Lu, Global analysis of charmless B decays into two vector mesons in soft-collinear effective theory, Phys. Rev. D **96**, 073004 (2017).

[64] C. Wang, Q. A. Zhang, Y. Li, and C. D. Lu, Charmless $B_{(s)} \to VV$ decays in factorization-assisted topological-amplitude approach, Eur. Phys. J. C **77**, 333 (2017).

[65] D. C. Yan, X. Liu, and Z. J. Xiao, Anatomy of $B_s \to VV$ decays and effects of next-to-leading order contributions in the perturbative QCD factorization approach, Nucl. Phys. **B935**, 17 (2018).

[66] Z. Rui, Y. Li, and H. Li, Studies of the resonance components in the B_s decays into charmonia plus kaon pair, Eur. Phys. J. C **79**, 792 (2019).

[67] Y. Li, D. C. Yan, J. Hua, Z. Rui, and H. n. Li, Global determination of two-meson distribution amplitudes from three-body B decays in the perturbative QCD approach, Phys. Rev. D **104**, 096014 (2021).

[68] S. Cheng, A. Khodjamirian, and J. Virto, Timelike-helicity $B \to \pi\pi$ form factor from light-cone sum rules with dipion distribution amplitudes, Phys. Rev. D **96**, 051901(R) (2017).

[69] C. Hambrock and A. Khodjamirian, Form factors in $\bar{B}^0 \to \pi^+\pi^0 l\bar{\nu}_l$ from QCD light-cone sum rules, Nucl. Phys. **B905**, 373 (2016).

[70] H.-Y. Cheng, C.-K. Chua, and K.-C. Yang, Charmless hadronic B decays involving scalar mesons: Implications on the nature of light scalar mesons, Phys. Rev. D **73**, 014017 (2006).

[71] H.-Y. Cheng, C.-K. Chua, and K.-C. Yang, Charmless B decays to a scalar meson and a vector meson, Phys. Rev. D **77**, 014034 (2008).

[72] M. K. Jia, C. Q. Zhang, J. M. Li, and Z. Rui, S-wave contributions to the $B_{(s)} \to \chi_{c1}(\pi\pi, K\pi, KK)$ decays, Phys. Rev. D **104**, 073001 (2021).

[73] D. Aston *et al.* (LASS Collaboration), A study of $K^-\pi^+$ scattering in the reaction $K^- p \to K^-\pi^+ n$ at 11 GeV/c, Nucl. Phys. **B296**, 493 (1988).

[74] R. Aaij *et al.* (LHCb Collaboration), Amplitude analysis of $B^0 \to \bar{D}^0 K^+\pi^-$ decays, Phys. Rev. D **92**, 012012 (2015).

[75] S. M. Flatte, On the nature of 0^+ mesons, Phys. Lett. **63B**, 228 (1976).

[76] R. Aaij *et al.* (LHCb Collaboration), Measurement of resonant and CP components in $\bar{B}_s^0 \to J/\psi\pi^+\pi^-$ decays, Phys. Rev. D **89**, 092006 (2014).

[77] D. V. Bugg, Reanalysis of data on $a_0(1450)$ and $a_0(980)$, Phys. Rev. D **78**, 074023 (2008).

[78] Y. Li, Z. Rui, and Z. J. Xiao, P-wave contributions to $B_{(s)} \to \psi K\pi$ decays in perturbative QCD approach, Chin. Phys. C **44**, 073102 (2020).

[79] Y. Li, D. C. Yan, Z. Rui, and Z.-J. Xiao, S, P and D-wave resonance contributions to $B_{(s)} \to \eta_c(1S, 2S)K\pi$ decays in the pQCD approach, Phys. Rev. D **101**, 016015 (2020).

[80] H. n. Li, QCD aspects of exclusive B meson decays, Prog. Part. Nucl. Phys. **51**, 85 (2003).

[81] T. Kurimoto, H. n. Li, and A. I. Sanda, Leading power contributions to $B \to \pi, \rho$ transition form-factors, Phys. Rev. D **65**, 014007 (2001).

[82] J. Hua, H. n. Li, C. D. Lu, W. Wang, and Z. P. Xing, Global analysis of hadronic two-body B decays in the perturbative QCD approach, Phys. Rev. D **104**, 016025 (2021).

[83] W. Wang, Y. M. Wang, J. Xu, and S. Zhao, B-meson light-cone distribution amplitude from the Euclidean quantities, Phys. Rev. D **102**, 011502(R) (2020).
[84] H. n. Li and H. S. Liao, B meson wave function in k_T factorization, Phys. Rev. D **70**, 074030 (2004).
[85] H. n. Li, Y. L. Shen, and Y. M. Wang, Resummation of rapidity logarithms in B meson wave functions, J. High Energy Phys. 02 (2013) 008.
[86] H. n. Li and Y. M. Wang, Non-dipolar Wilson links for transverse-momentum-dependent wave functions, J. High Energy Phys. 06 (2015) 013.
[87] H. n. Li, Y. L. Shen, and Y. M. Wang, Next-to-leading-order corrections to $B \to \pi$ form factors in k_T factorization, Phys. Rev. D **85**, 074004 (2012).
[88] Y. K. Hsiao and C. Q. Geng, Four-body baryonic decays of $B \to p\bar{p}\pi^+\pi^-(\pi^+K^-)$ and $\Lambda\bar{p}\pi^+\pi^-(K^+K^-)$, Phys. Lett. B **770**, 348 (2017).
[89] C. s. Kim, Y. Li, and W. Wang, Study of decay modes $B \to K_0^*(1430)\phi$, Phys. Rev. D **81**, 074014 (2010).
[90] J. P. Lees *et al.* (*BABAR* Collaboration), B^0 meson decays to $\rho^0 K^{*0}$, $f_0 K^{*0}$, and $\rho^- K^{*+}$, including higher K^* resonances, Phys. Rev. D **85**, 072005 (2012).
[91] S. H. Kyeong *et al.* (Belle Collaboration), Measurements of charmless hadronic $b \to s$ penguin decays in the $\pi^+\pi^-K^+\pi^-$ final state and observation of $B^0 \to \rho^0 K^+\pi^-$, Phys. Rev. D **80**, 051103 (2009).
[92] M. Ablikim *et al.* (BES Collaboration), Partial wave analysis of $\chi_{c0} \to \pi^+\pi^-K^+K^-$, Phys. Rev. D **72**, 092002 (2005).
[93] H. Y. Cheng, C. W. Chiang, and C. K. Chua, Finite-width effects in three-body B decays, Phys. Rev. D **103**, 036017 (2021).
[94] H. Y. Cheng, C. W. Chiang, and C. K. Chua, Width effects in resonant three-body decays: B decay as an example, Phys. Lett. B **813**, 136058 (2021).
[95] Q. Chang, X. Li, X. Q. Li, and J. Sun, Study of the weak annihilation contributions in charmless $B_s \to VV$ decays, Eur. Phys. J. C **77**, 415 (2017).
[96] E. Alvarez, L. N. Epele, D. Gomez Dumm, and A. Szynkman, Right handed currents and FSI phases in $B^0 \to \phi K^{*0}$, Phys. Rev. D **70**, 115014 (2004).
[97] K. C. Yang, Annihilation in factorization-suppressed B decays involving a 1^1P_1 meson and search for new-physics signals, Phys. Rev. D **72**, 034009 (2005); Erratum, **72**, 059901 (2005).
[98] S. Baek, A. Datta, P. Hamel, O. F. Hernandez, and D. London, Polarization states in $B \to \rho K^*$ and new physics, Phys. Rev. D **72**, 094008 (2005).
[99] C. S. Huang, P. Ko, X. H. Wu, and Y. D. Yang, MSSM anatomy of the polarization puzzle in $B \to \phi K^*$ decays, Phys. Rev. D **73**, 034026 (2006).
[100] C. H. Chen and H. Hatanaka, Nonuniversal Z' couplings in B decays, Phys. Rev. D **73**, 075003 (2006).
[101] A. Faessler, T. Gutsche, J. C. Helo, S. Kovalenko, and V. E. Lyubovitskij, Possible resolution of the B-meson decay polarization anomaly in R-parity violating SUSY, Phys. Rev. D **75**, 074029 (2007).
[102] C. H. Chen, C. Q. Geng, Y. K. Hsiao, and Z. T. Wei, Productions of $K_0^*(1430)$ and K_1 in B decays, Phys. Rev. D **72**, 054011 (2005).
[103] C. H. Chen and C. Q. Geng, Expectations on $B \to (K_0^*(1430), K_2^*(1430))\phi$ decays, Phys. Rev. D **75**, 054010 (2007).
[104] H. Y. Cheng and K. C. Yang, Charmless hadronic B decays into a tensor meson, Phys. Rev. D **83**, 034001 (2011).
[105] C. Bobeth, M. Gorbahn, and S. Vickers, Weak annihilation and new physics in charmless $B \to MM$ decays, Eur. Phys. J. C **75**, 340 (2015).
[106] H. Y. Cheng and C. K. Chua, Revisiting charmless hadronic $B_{u,d}$ decays in QCD factorization, Phys. Rev. D **80**, 114008 (2009).
[107] B. Aubert *et al.* (*BABAR* Collaboration), Amplitude Analysis of the $B^\pm \to \phi K^*(892)^\pm$ Decay, Phys. Rev. Lett. **99**, 201802 (2007).